

Electronic supporting information

Series of High Spin Mononuclear Iron(III) Complexes with Schiff Base ligands derived from 2-hydroxybenzophenones

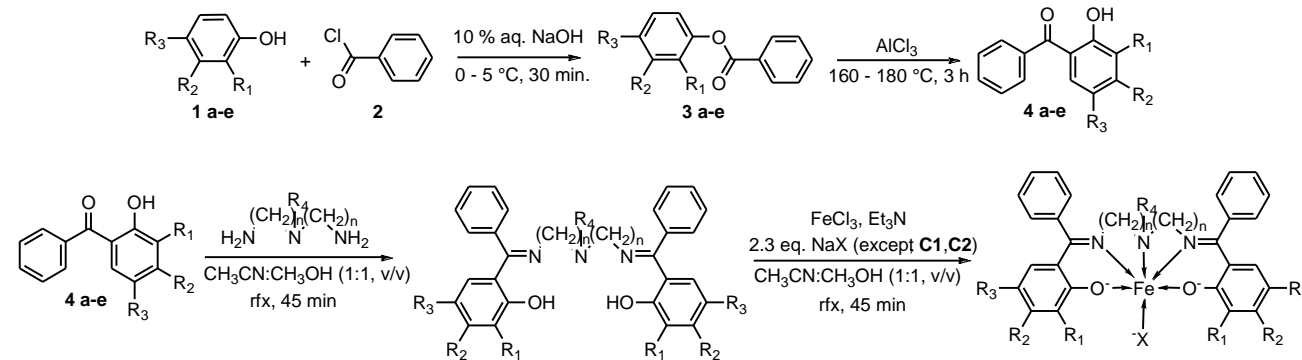
Lukáš Pogány,^{a*} Ján Moncol,^a Ján Pavlik,^a and Ivan Šalitroš,^a

a) Department of Inorganic Chemistry, Faculty of Chemical and Food Technology, Slovak University of Technology in Bratislava, Bratislava SK-81237, Slovakia, *e-mail: lukas.pogany@stuba.sk

Contents

S1 Scheme of syntheses, synthetic protocols and spectral characterization	2
S2 FTIR spectroscopy of reported compounds	7
S3 UV-VIS spectroscopy of reported compounds	17
S4 ¹ H and ¹³ C NMR spectroscopy of reported compounds	18
S5 Crystallographic data, bond angles and metric parameter of coordination polyhedra	28
S6 Magnetic functions and their theoretical analyses	36

S1 Scheme of syntheses, synthetic protocols and spectral characterization



	R ₁	R ₂	R ₃		R ₁	R ₂	R ₃	R ₄	n	X		R ₁	R ₂	R ₃	R ₄	n	X		
a	H	H	CH ₃		C1	H	H	CH ₃	H	2	Cl		C6	H	H	Cl	H	2	NCO
b	CH ₃	H	CH ₃		C2	CH ₃	H	CH ₃	H	2	Cl		C7	H	CH ₃	H	H	2	N ₃
c	H	H	Cl		C3	CH ₃	H	CH ₃	H	2	N ₃		C8	H	H	Br	H	3	N ₃
d	H	CH ₃	H		C4	CH ₃	H	CH ₃	H	2	NCO		C9	H	H	Br	CH ₃	3	N ₃
e	H	H	Br		C5	H	H	Cl	H	2	N ₃								

Fig. S1 Upper: Scheme of preparation of substituted phenyl benzoate (3 a-e) and corresponding derivative of 2-hydroxybenzophenone (4 a-e). For **a** R₁ = R₂ = H, R₃ = CH₃; for **b** R₁ = R₃ = CH₃, R₂ = H; for **c** R₁ = R₂ = H, R₃ = Cl; for **d** R₁ = R₃ = H, R₂ = CH₃; for **e** R₁ = R₂ = H, R₃ = Br. Bottom: Scheme of syntheses of Schiff base ligands H₂L_n and complexes **C1-C9**. For **C1** (and corresponding ligand H₂L₁) R₁ = R₂ = R₄ = H, R₃ = CH₃, n = 2, X = Cl; for **C2-C4** (and corresponding ligand H₂L₂) R₁ = R₃ = CH₃, R₂ = R₄ = H, n = 2 and X = Cl (**C2**), N₃ (**C3**) or NCO (**C4**); for **C5** and **C6** (and corresponding ligand H₂L₃) R₁ = R₂ = R₄ = H, R₃ = Cl, n = 2 and X = N₃ (**C5**) or NCO (**C6**); for **C7** (and corresponding ligand H₂L₄) R₁ = R₃ = R₄ = H, R₂ = CH₃, n = 2 and X = N₃; for **C8** (and corresponding ligand H₂L₅) R₁ = R₂ = R₄ = H, R₃ = Br, n = 3 and X = N₃; for **C9** (and corresponding ligand H₂L₆) R₁ = R₂ = H, R₃ = Br, R₄ = CH₃, n = 3 and X = N₃.

Synthesis and spectral properties of phenyl benzoates derivatives

4-methylphenyl benzoate (3a): The Erlenmayer flask was charged with 4-methylphenol (10.8 g, 100 mmol), water (150 mL) and 10 % sodium hydroxide solution (60 mL). Ice (ca. 150 g) was added to the solution and benzoyl chloride (11.6 mL, 100 mmol) was poured in small portions while the reaction mixture was vigorously stirred. The product that solidified upon stirring as off-white solid was filtered off and washed with water (200 mL). Isothermal crystallization from ethanol with activated charcoal afforded product in white polycrystalline powder in 77 % yield. ¹H NMR (500 MHz, CDCl₃, 25 °C, δ/ppm): 8.20-8.18 (dd, J₁ = 8.2 Hz, J₂ = 1.2 Hz, 2H), 7.62-7.58 (t, J=7.5 Hz, 1H), 7.50-7.47 (t, J=8.0 Hz 2H), 7.21-7.20 (d, J=8.5 Hz, 2H), 7.10-7.08 (d, J= 6.50 Hz, 2H), 2.36 (s, 3H). ¹³C NMR (125 MHz, CDCl₃, 25 °C, δ/ppm): 165.6, 149.0, 135.8, 133.8, 130.4, 130.3, 130.0, 128.8, 121.7, 21.2. FT-IR (ATR, $\tilde{\nu}_{\text{max}}/\text{cm}^{-1}$): 3072 (w, C-H_{ar}), 3039 (w, C-H_{ar}), 2924(w, C-H_{alif}), 1724 (s, C=O). UV-VIS (nujol, $\lambda_{\text{max}}/\text{nm}$): 282, 272, 232. Elemental analysis for C₁₄H₁₂O₂: Found % (Calc. %): C 80.04 (79.22), H 5.96 (5.70).

2,4-dimethylphenyl benzoate (3b): 4-methylphenyl benzoate (**3b**) was prepared in the same manner as **3a**, however, 2,4-dimethylphenol (**1b**, 12.2 g, 100 mmol) was used instead of **1a**. Isothermal crystallization from ethanol after purification with activated charcoal afforded product in white polycrystalline powder in 80 % yield. ¹H NMR (500 MHz, CDCl₃, 25 °C, δ/ppm): 8.26-8.24 (d, J=7.5 Hz, 2H), 7.67-7.63 (t, J=7.5 Hz, 1H), 7.55-7.52 (t, J=7.8Hz, 2H), 7.11-7.03 (m, 3H), 2.36 (s, 3H), 2.22 (s, 3H). ¹³C NMR (125 MHz, CDCl₃, 25 °C, δ/ppm): 165.4, 147.6, 136.0, 133.8, 132.1, 130.5, 130.1, 129.9, 128.9, 127.8, 122.0, 21.2, 16.5. FT-IR (ATR, $\tilde{\nu}_{\text{max}}/\text{cm}^{-1}$): 3006(w, C-H_{ar}), 2920 (w, C-H_{alif}), 1724 (s, C=O). UV-VIS (nujol, $\lambda_{\text{max}}/\text{nm}$): 282, 273, 233. Elemental analysis for C₁₅H₁₄O₂: Found % (Calc. %): C 80.13 (79.62), H 6.36 (6.24).

4-chlorophenyl benzoate (3c): 4-chlorophenyl benzoate (**3c**) was prepared in the same manner as **3a**, but 4-chlorophenol (**1c**, 12.9 g, 100 mmol) was used instead of **1a**. Isothermal crystallization from ethanol with after purification with activated charcoal afforded product in white polycrystalline powder in 72 % yield. ¹H NMR (500 MHz, CDCl₃, 25 °C, δ/ppm): 8.21-8.20 (d, J=7.5 Hz, 2H), 7.67-7.64 (t, J=7.5 Hz, 1H), 7.54-7.51 (t, J=7.8 Hz, 2H), 7.42-7.39 (m, 2H), 7.20-7.17 (m, 2H). ¹³C NMR (125 MHz, CDCl₃, 25 °C, δ/ppm): 165.3, 149.7, 134.1, 131.6, 130.5, 129.9, 129.5, 129.0, 123.4. FT-IR (ATR, $\tilde{\nu}_{\text{max}}/\text{cm}^{-1}$): 3063 (w, C-H_{ar}), 1731 (s, C=O). UV-VIS (nujol, $\lambda_{\text{max}}/\text{nm}$): 284, 276, 234. Elemental analysis for C₁₄H₉ClO₂: Found % (Calc. %): C 67.56 (67.11), H 3.91 (3.90).

3-methylphenyl benzoate (3d): 3-methylphenyl benzoate (**3d**) was prepared in the same manner as **3a**, however, 3-methylphenol (**1d**, 10.8 g, 100 mmol) was used instead of **1a**. Isothermal crystallization from ethanol after purification with activated charcoal afforded product in white polycrystalline powder in 82 % yield. ¹H NMR (500 MHz, CDCl₃, 25 °C, δ/ppm): 8.26-8.24 (d, J=6.5 Hz,

2H), 7.67-7.64 (t, J=7.5 Hz, 1H), 7.55-7.52 (t, J=7.8 Hz, 2H), 7.36-7.33 (t, J=7.8 Hz, 1H), 7.13-7.11 (d, J=8.0 Hz, 1H), 7.08-7.05 (m, 2H), 2.43 (s, 3H). ^{13}C NMR (125 MHz, CDCl_3 , 25 °C, δ/ppm): 165.5, 151.2, 139.9, 133.8, 130.4, 129.9, 129.5, 128.8, 127.0, 122.6, 118.9, 21.6. FT-IR (ATR, $\tilde{\nu}_{\text{max}}/\text{cm}^{-1}$): 3040 (w, C-H_{ar}), 2917 (w, C-H_{alif}), 1730 (s, C=O). UV-VIS (nujol, $\lambda_{\text{max}}/\text{nm}$): 280, 276, 233. Elemental analysis for $\text{C}_{14}\text{H}_{12}\text{O}_2$: Found % (Calc. %): C 79.93 (79.22), H 5.79 (5.70).

4-bromophenyl benzoate (3e): 4-bromophenyl benzoate (**3e**) was prepared in the same manner as **3a**, but 4-bromophenol (**1e**, 17.3 g, 100 mmol) was used instead of **1a**. Isothermal crystallization from ethanol after purification with activated charcoal afforded product in white polycrystalline powder in 85 % yield. ^1H NMR (500 MHz, CDCl_3 , 25 °C, δ/ppm): 8.21-8.19 (d, J=7.5 Hz, 2H), 7.67-7.64 (t, J=7.5 Hz, 1H), 7.57-7.51 (m, 4H), 7.14-7.11 (d, J=9.0 Hz, 2H). ^{13}C NMR (125 MHz, CDCl_3 , 25 °C, δ/ppm): 165.2, 150.3, 134.1, 132.9, 130.5, 129.5, 129.0, 123.9, 119.3. FT-IR (ATR, $\tilde{\nu}_{\text{max}}/\text{cm}^{-1}$): 3062 (w, C-H_{ar}), 1728 (s, C=O). UV-VIS (nujol, $\lambda_{\text{max}}/\text{nm}$): 284, 277, 234. Elemental analysis for $\text{C}_{14}\text{H}_9\text{BrO}_2$: Found % (Calc. %): C 56.42 (56.34), H 3.18 (3.27).

Synthesis and spectral properties of 2-hydroxybenzophenone derivatives

2-hydroxy-5-methylbenzophenone (4a): 250 ml round-bottom flask was charged with 4-methylphenyl benzoate (**3a**, 21.2 g, 100 mmol, 1 eq.) and anhydrous aluminium chloride (16.7 g, 125 mmol, 1.25 eq.). The melted reaction mixture was slowly stirred at 160-180 °C for 3 hours, cooled down to room temperature and quenched with ice-cold water (170 mL) and 10 % aqueous solution of hydrochloric acid (85 mL). Dichloromethane (200 mL) was added and mixture was shaken well until it completely dissolved. The solution was transferred to a separatory funnel, aqueous layer was separated from the organic one and extracted two more times (2x200 mL). Combined organic layers were concentrated to ca. 150 mL under reduced pressure, transferred back to separatory funnel and extracted with 2.5 % sodium hydroxide solution (4x250 mL). Combined alkaline water layers were acidified with 10 % sulphuric acid (pH ≈ 1, ca 300 mL). The product that precipitates as yellow crystalline solid was filtered off and dried in the air. Isothermal crystallization from methanol after purification with activated charcoal afforded product **4a** as yellow polycrystalline powder in 70 % yield. ^1H NMR (500 MHz, CDCl_3 , 25 °C, δ/ppm): 11.88 (s, 1H), 7.68-7.67 (d, J=6.5 Hz, 2H), 7.61-7.58 (t, J=7.5 Hz, 1H), 7.53-7.50 (t, J=7.5 Hz, 2H), 7.37 (s, 1H), 7.34-7.32 (dd, $J_1 = 8.5$ Hz, $J_2 = 2.0$ Hz, 1H), 7.00-6.98 (d, J=8.5 Hz, 1H), 2.26 (s, 3H). ^{13}C NMR (125 MHz, CDCl_3 , 25 °C, δ/ppm): 201.9, 161.4, 138.3, 137.7, 133.5, 132.1, 129.4, 128.6, 128.1, 119.1, 118.4, 20.8. FT-IR (ATR, $\tilde{\nu}_{\text{max}}/\text{cm}^{-1}$): 3055 (w, C-H_{ar}), 2916 (w, C-H_{alif}), 1626 (s, C=O). UV-VIS (nujol, $\lambda_{\text{max}}/\text{nm}$): 353, 259, 222. Elemental analysis for $\text{C}_{14}\text{H}_{12}\text{O}_2$: Found % (Calc. %): C 79.71 (79.22), H 5.78 (5.70).

2-hydroxy-3,5-dimethylbenzophenone (4b): 2-hydroxy-3,5-dimethylbenzophenone (**4b**) was prepared in the same manner as **4a**, however, 2,4-dimethylphenyl benzoate (**3b**, 22.6 g, 100 mmol) was used instead of **3a**. The product that separated after acidification of alkaline water layer as yellow oil was separated by extraction with dichloromethane (3x500 mL), combined organic layers were dried with anhydrous magnesium sulphate and concentrated on rotary evaporator to dryness. The yellow oil was dissolved in methanol, purified with activated charcoal and the solution was set for isothermal crystallization that afforded product in yellow polycrystalline powder in 78% yield. ¹H NMR (500 MHz, CDCl₃, 25 °C, δ/ppm): 12.17 (s, 1H), 7.67-7.66 (d, J=7.0 Hz, 2H), 7.60-7.57 (t, J=7.3 Hz, 1H), 7.52-7.49 (t, J=7.8 Hz, 2H), 7.21-7.20 (m, 2H), 2.30 (s, 3H), 2.22 (s, 3H). ¹³C NMR (125 MHz, CDCl₃, 25 °C, δ/ppm): 202.2, 159.9, 138.8, 138.7, 132.0, 131.2, 129.4, 128.6, 127.5, 127.3, 118.5, 20.8, 15.9. FT-IR (ATR, $\tilde{\nu}_{\text{max}}/\text{cm}^{-1}$): 3055 (w, C-H_{ar}), 2914 (w, C-H_{alif}), 1614 (s, C=O). UV-VIS (nujol, $\lambda_{\text{max}}/\text{nm}$): 362, 265, 218. Elemental analysis for C₁₅H₁₄O₂: Found % (Calc. %): C 80.13 (79.62); H 6.35 (6.24).

5-chloro-2-hydroxybenzophenone (4c): 5-chloro-2-hydroxybenzophenone (**4c**) was prepared in the same manner as **4a**, however, 4-chlorophenyl benzoate (**3c**, 23.3 g, 100 mmol) was used instead of **3a**. Isothermal crystallization from methanol after purification with activated charcoal afforded product in yellow polycrystalline powder in 78 % yield. ¹H NMR (500 MHz, CDCl₃, 25 °C, δ/ppm): 11.92 (s, 1H), 7.68-7.67 (d, J=7.0 Hz, 2H), 7.64-7.61 (t, J=7.5 Hz, 1H), 7.56-7.52 (m, 3H), 7.47-7.44 (dd, J₁ = 9.0 Hz, J₂ = 2.5 Hz, 1H), 7.05-7.03 (d, J=9.0 Hz, 1H). ¹³C NMR (125 MHz, CDCl₃, 25 °C, δ/ppm): 201.0, 162.0, 137.5, 136.5, 132.7, 129.5, 128.9, 123.7, 120.4, 120.0. FT-IR (ATR, $\tilde{\nu}_{\text{max}}/\text{cm}^{-1}$): 3070 (w, C-H_{ar}), 1623 (s, C=O). UV-VIS (nujol, $\lambda_{\text{max}}/\text{nm}$): 354, 262, 226. Elemental analysis for C₁₄H₉ClO₂: Found % (Calc. %): C 67.81 (67.11); H 3.68 (3.90).

2-hydroxy-4-methylbenzophenone (4d): 2-hydroxy-4-methylbenzophenone (**4d**) was prepared in the same manner as **4a**, however, starting with 3-methylphenyl benzoate (**3d**, 21.2 g, 100 mmol) instead of **3a**. **4d** separated after acidification of alkaline water layer as yellow oil and thus it was treated as **4b**. Isothermal crystallization from methanol after purification with activated charcoal afforded product in pale yellow polycrystalline powder in 40 % yield. ¹H NMR (500 MHz, CDCl₃, 25 °C, δ/ppm): 12.15 (s, 1H), 7.67-7.65 (d, J=7.0 Hz, 2H), 7.59-7.56 (t, J=6.3 Hz, 1H), 7.51-7.46 (m, 3H), 6.89 (s, 1H), 6.69-6.67 (dd, J₁ = 8.3 Hz, J₂ = 1.3 Hz, 1H), 2.38 (s, 3H). ¹³C NMR (125 MHz, CDCl₃, 25 °C, δ/ppm): 201.4, 163.7, 148.4, 138.4, 133.8, 132.0, 129.4, 128.6, 120.3, 118.8, 117.2, 22.3.; FT-IR (ATR, $\tilde{\nu}_{\text{max}}/\text{cm}^{-1}$): 3033 (w, C-H_{ar}), 2917 (w, C-H_{alif}), 1622 (s, C=O). UV-VIS (nujol, $\lambda_{\text{max}}/\text{nm}$): 339, 273, 219. Elemental analysis for C₁₄H₁₂O₂: Found % (Calc. %): C 79.43 (79.22), H 5.77 (5.70).

5-bromo-2-hydroxybenzophenone (4e): 5-bromo-2-hydroxybenzophenone (**4e**) was prepared in the same manner as **4a**, however, starting with 4-bromophenyl benzoate (**3c**, 27.7 g, 100 mmol) instead

of **3a**. Isothermal crystallization from methanol after purification with activated charcoal afforded product in yellow polycrystalline powder in 91 % yield. ¹H NMR (500 MHz, CDCl₃, 25 °C, δ/ppm): 11.93 (s, 1H), 7.71-7.67 (m, 3H), 7.65-7.62 (t, J= 7.5 Hz, 1H), 7.60-7.58 (dd, J₁ = 8.3 Hz, J₂ = 2.3 Hz, 1H), 7.56-7.53 (t, J= 7.8 Hz, 2H), 7.00-6.98 (d, J= 8.5 Hz, 1H). ¹³C NMR (125 MHz, CDCl₃, 25 °C, δ/ppm): 200.9, 162.5, 139.3, 137.5, 135.7, 132.8, 129.5, 129.0, 120.8, 120.7, 110.6. FT-IR (ATR, $\tilde{\nu}_{\text{max}}/\text{cm}^{-1}$): 3063 (w, C-H_{ar}), 1620 (s, C=O). UV-VIS (nujol, $\lambda_{\text{max}}/\text{nm}$): 355, 262, 226. Elemental analysis for C₁₄H₉BrO₂: Found % (Calc. %): C 56.43 (56.34), H 3.55 (3.27).

S2 FTIR spectroscopy of reported compounds

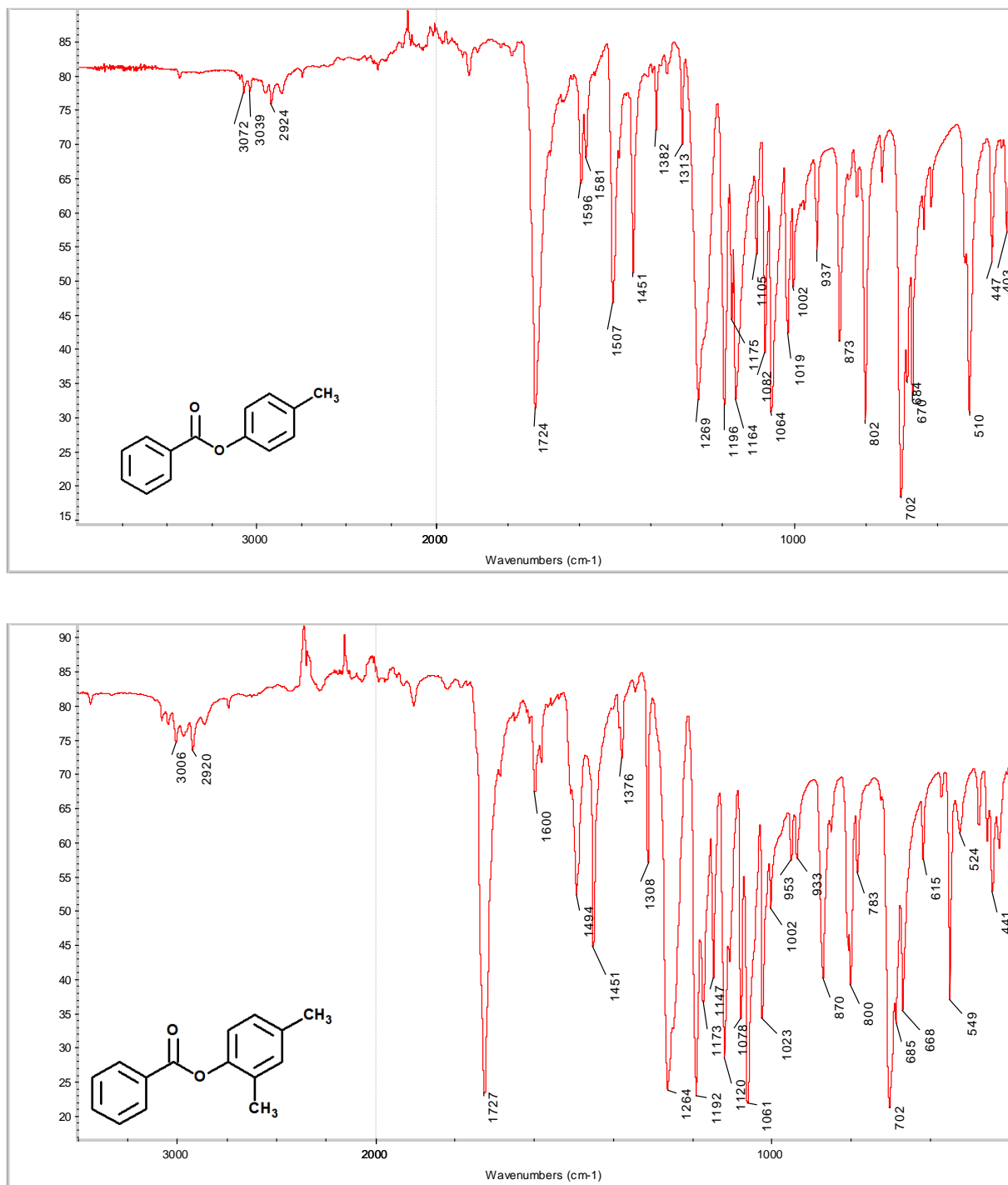


Fig. S2 FT-IR spectra of **3a** (upper) and **3b** (bottom)

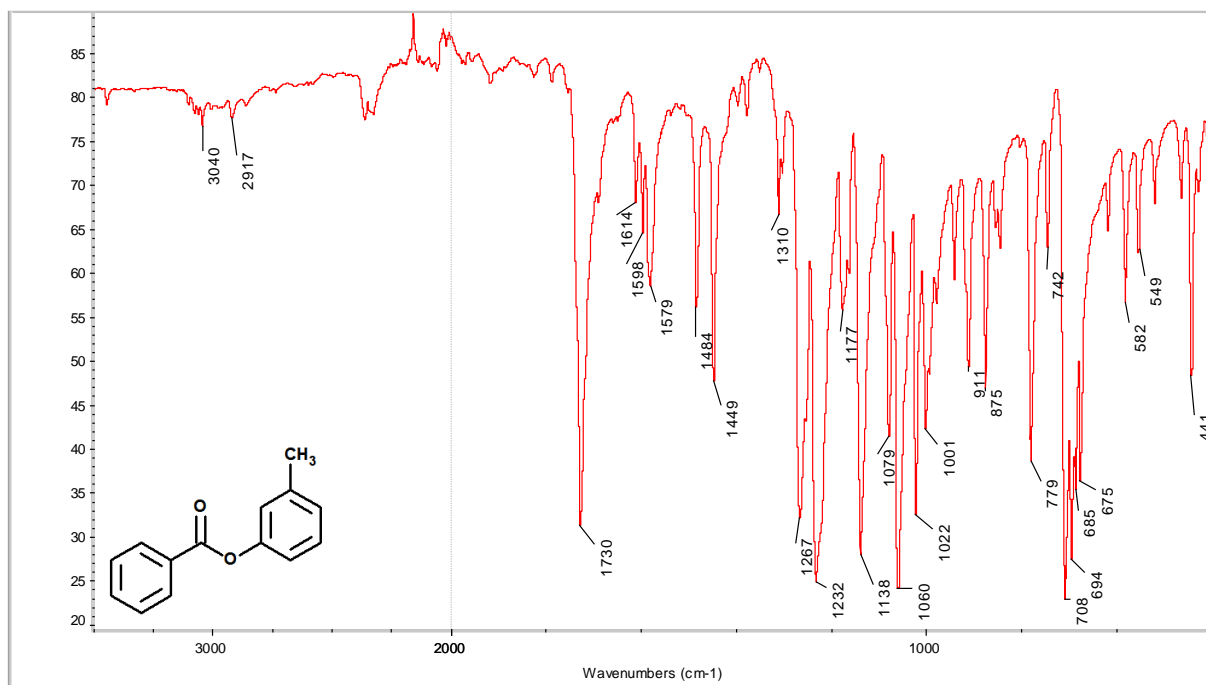
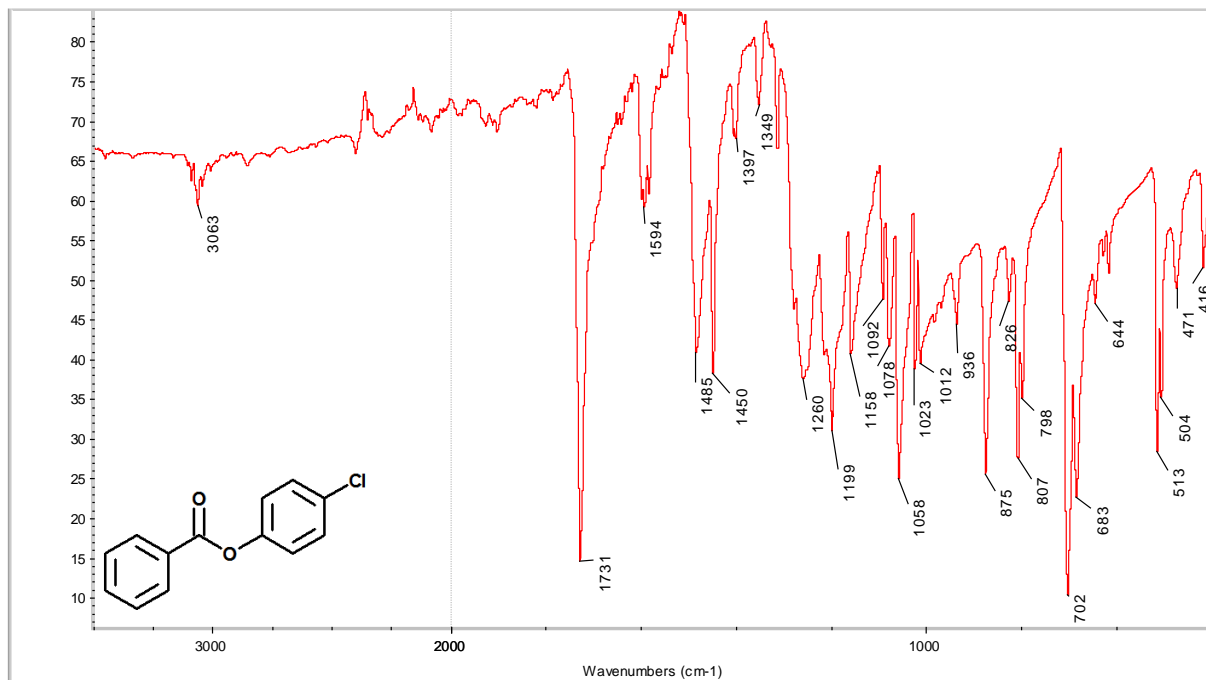


Fig. S3 FT-IR spectra of **3c** (upper) and **3d** (bottom)

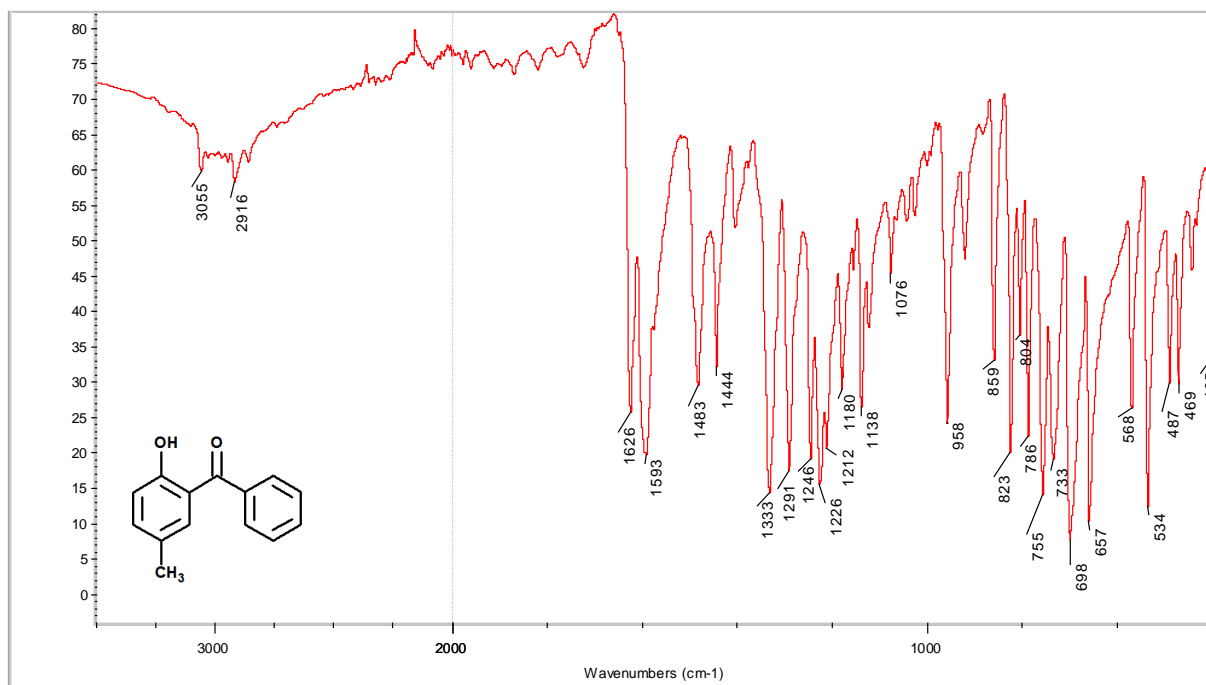
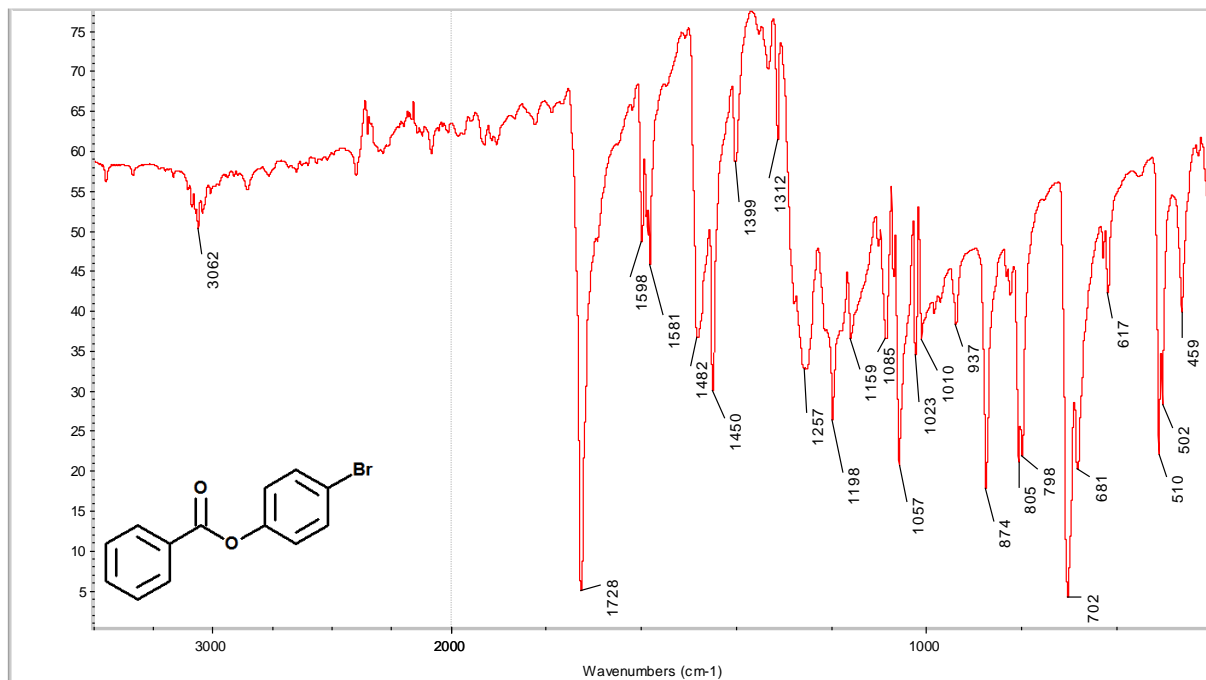


Fig. S4 FT-IR spectra of **3e** (upper) and **4a** (bottom)

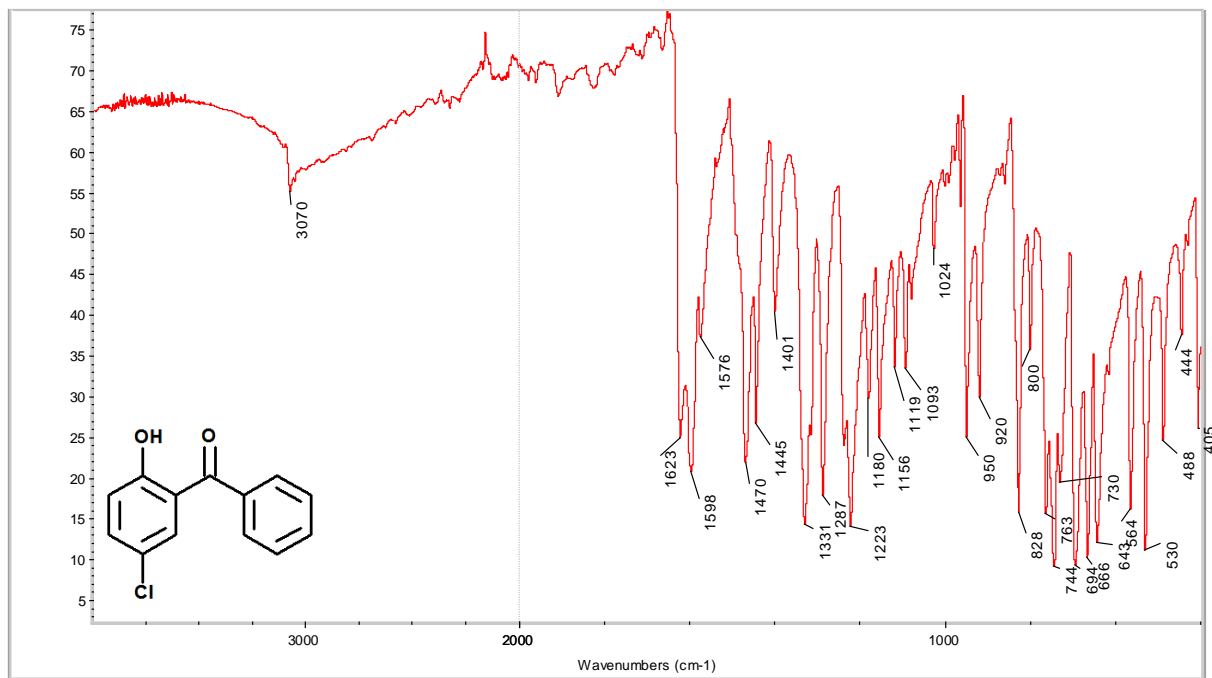
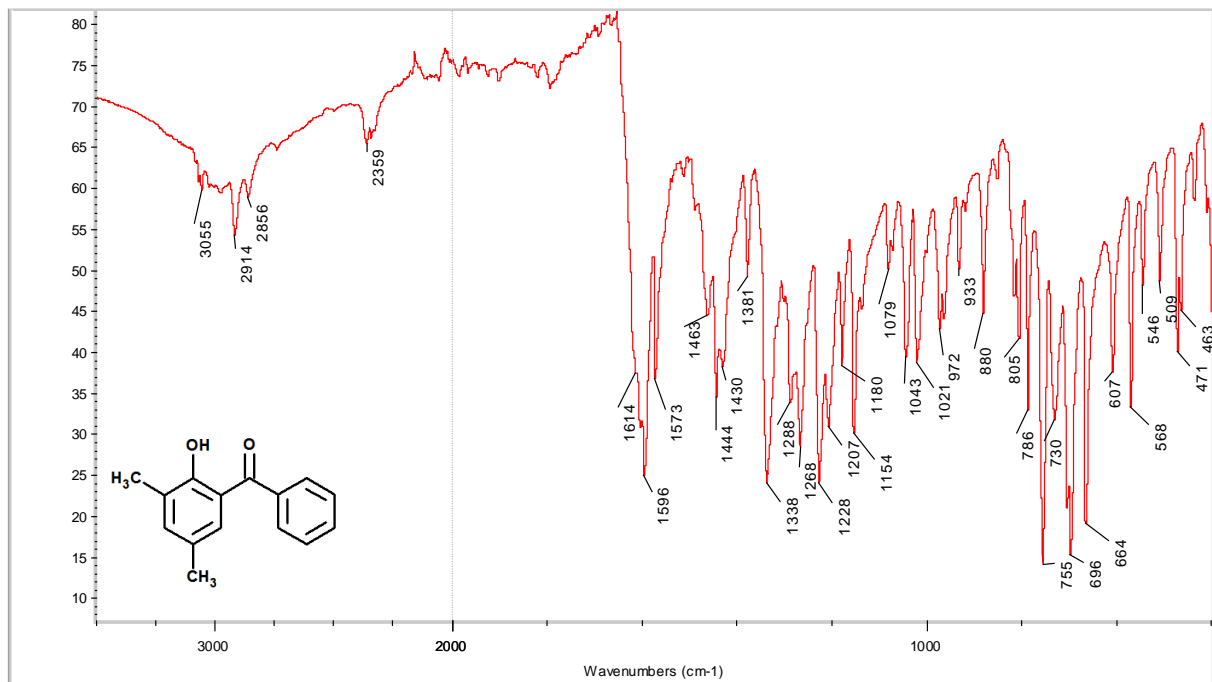


Fig. S5 FT-IR spectra of **4b** (upper) and **4c** (bottom)

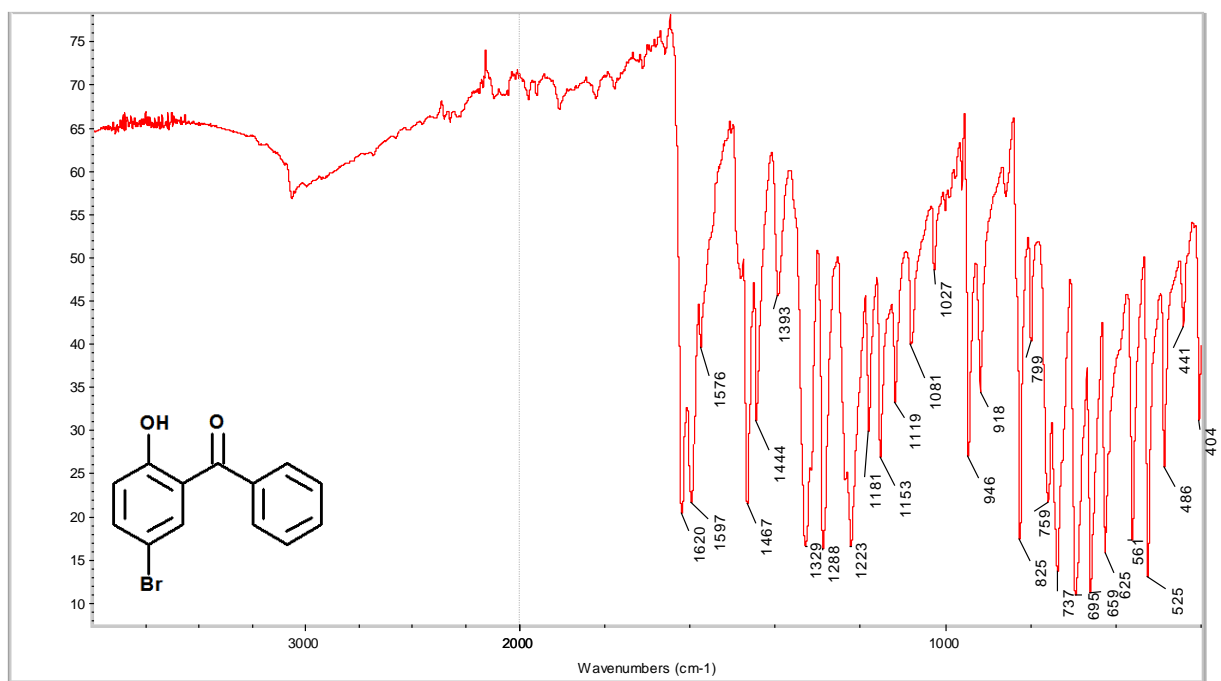
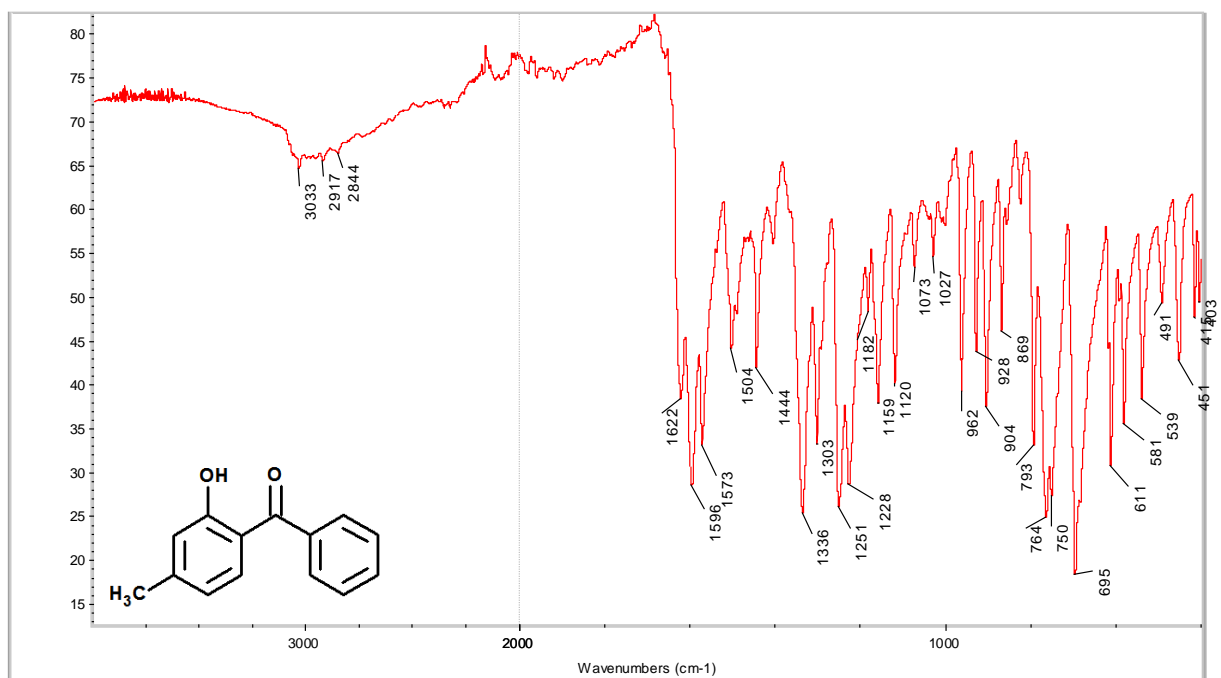


Fig. S6 FT-IR spectra of **4d** (upper) and **4e** (bottom)

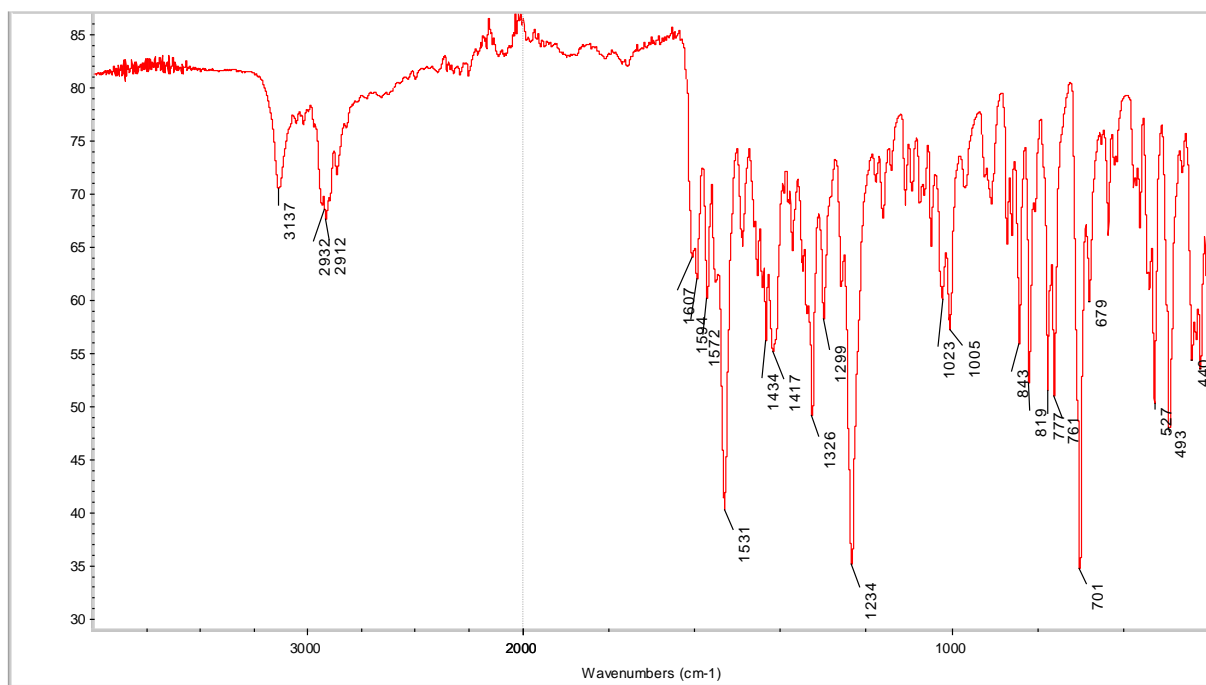
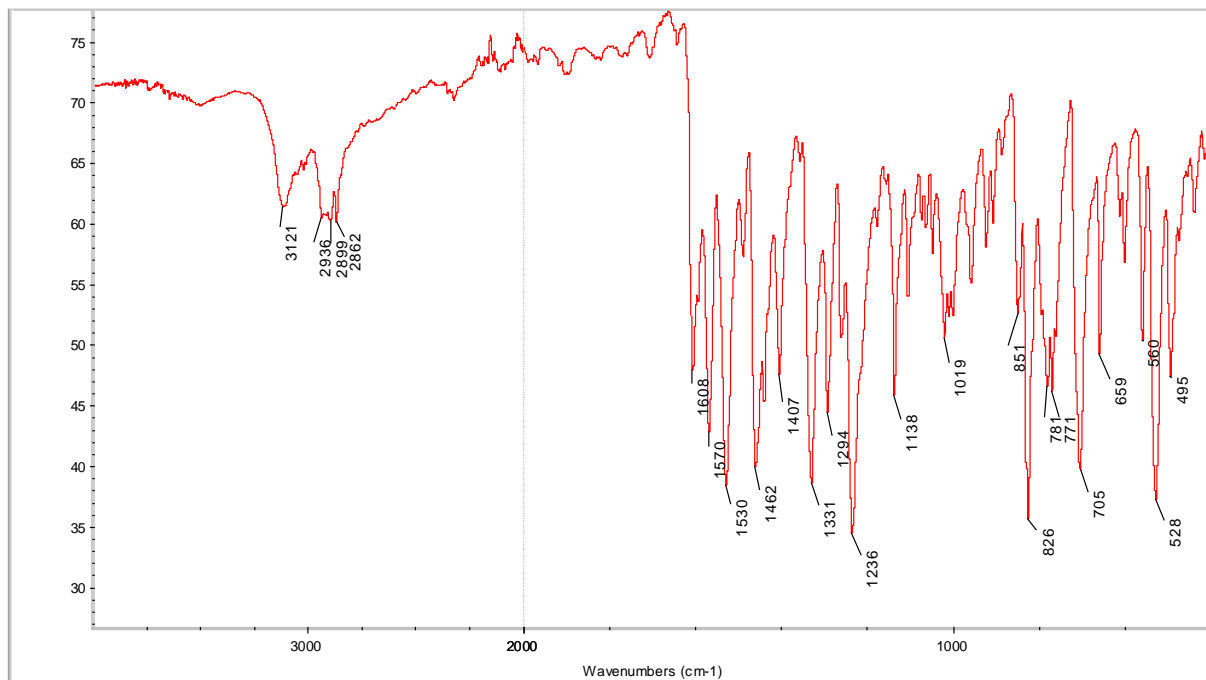


Fig. S7 FT-IR spectra of **C1** (upper) and **C2** (bottom)

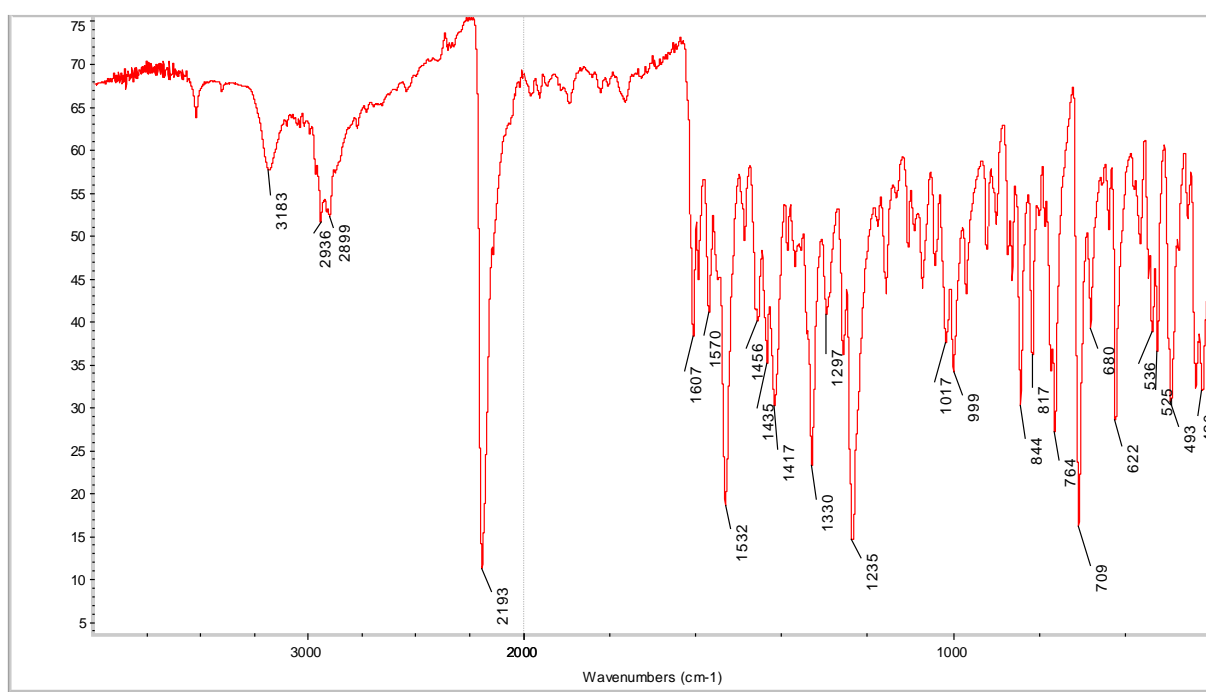
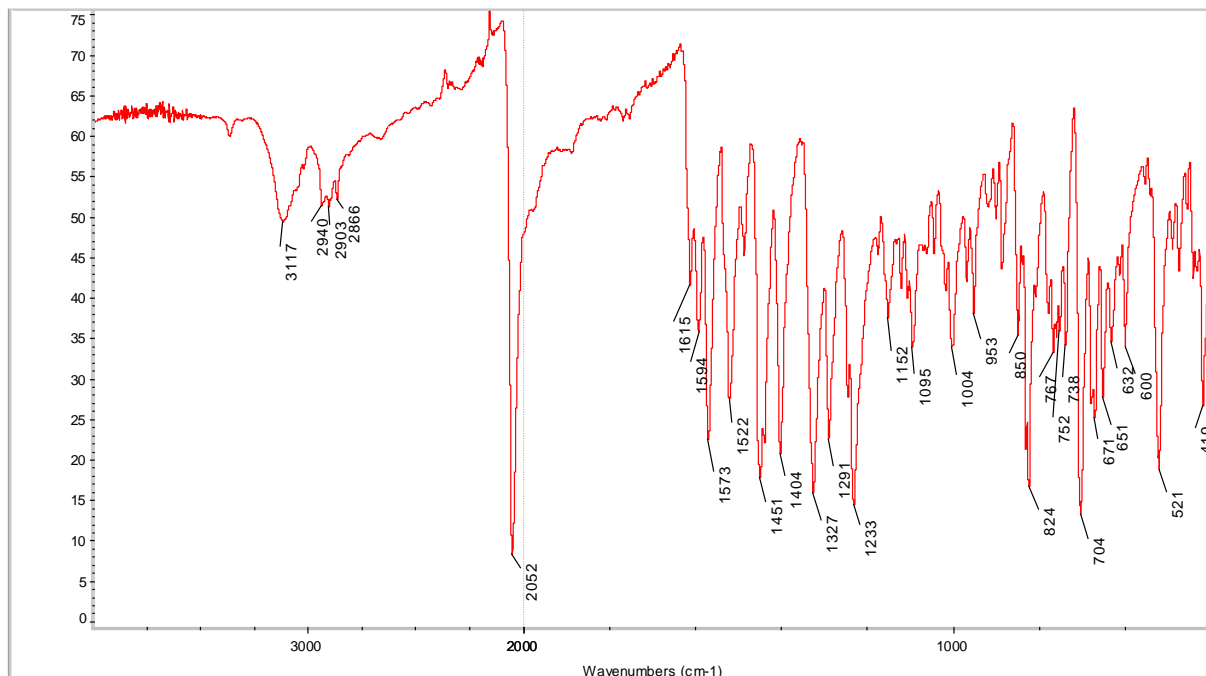


Fig. S8 FT-IR spectra of **C3** (upper) and **C4** (bottom)

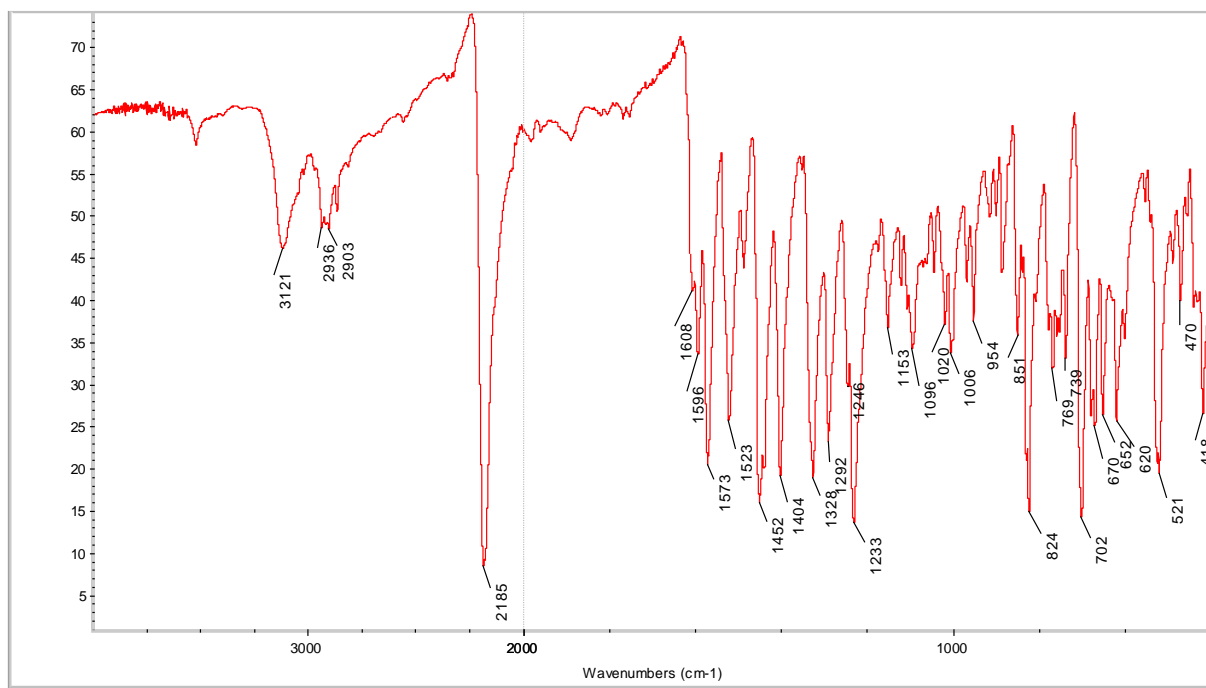
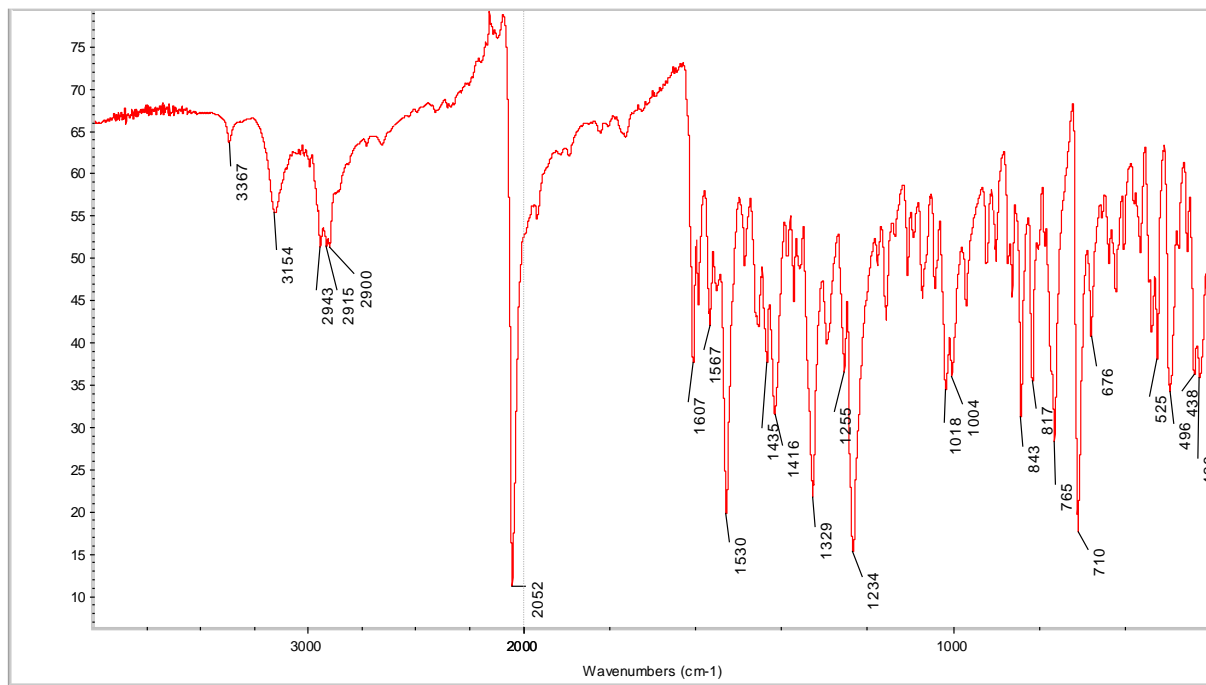


Fig. S9 FT-IR spectra of **C5** (upper) and **C6** (bottom)

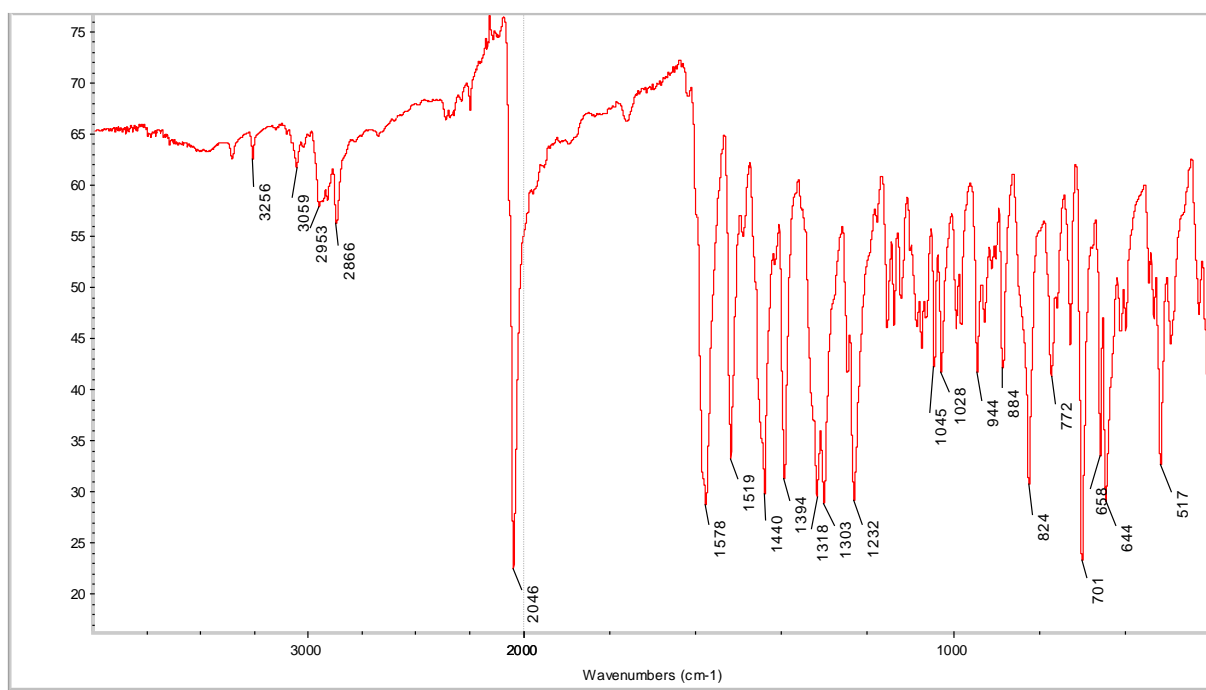
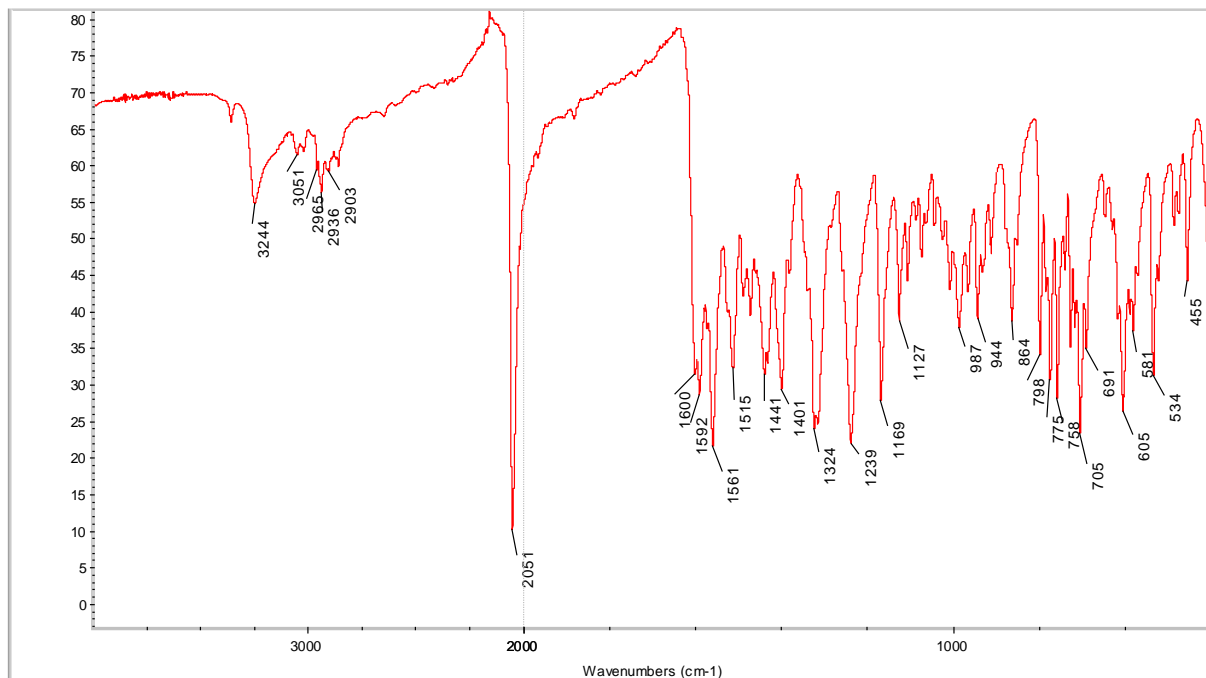


Fig. S10 FT-IR spectra of **C7** (upper) and **C8** (bottom)

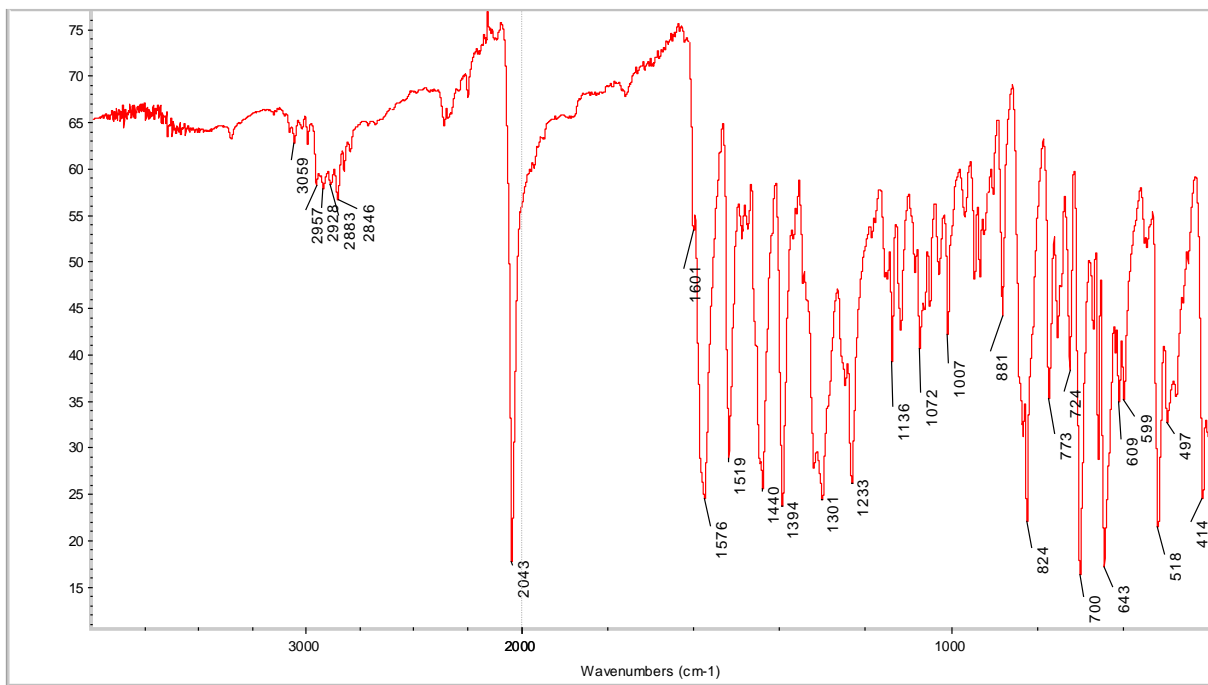


Fig. S11 FT-IR spectra of **C9**

S3 UV-VIS spectroscopy of reported compounds

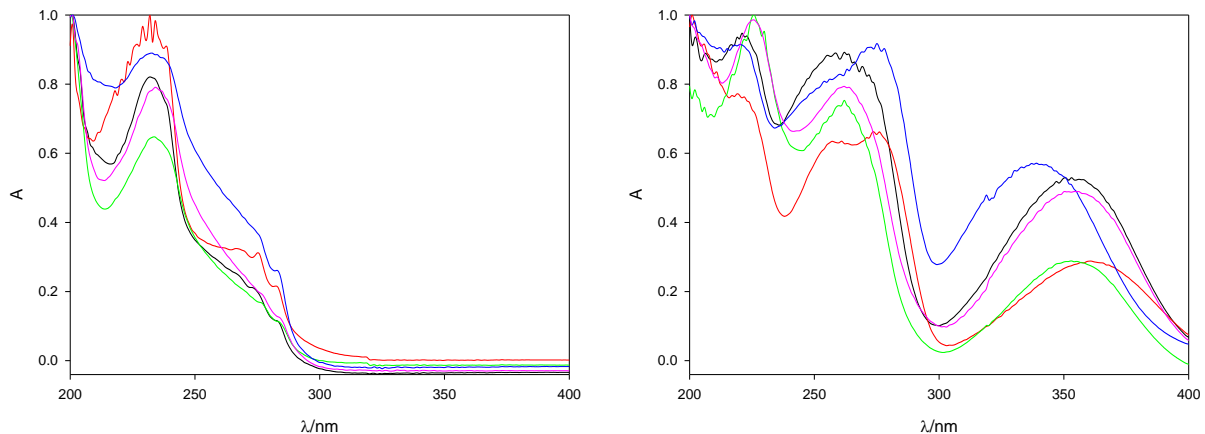


Fig. S12 Left: UV-VIS spectra of **3a** (black), **3b** (red), **3c** (green), **3d** (blue) and **3e** (pink). Right: UV-VIS spectra of **4a** (black), **4b** (red), **4c** (green), **4d** (blue) and **4e** (pink).

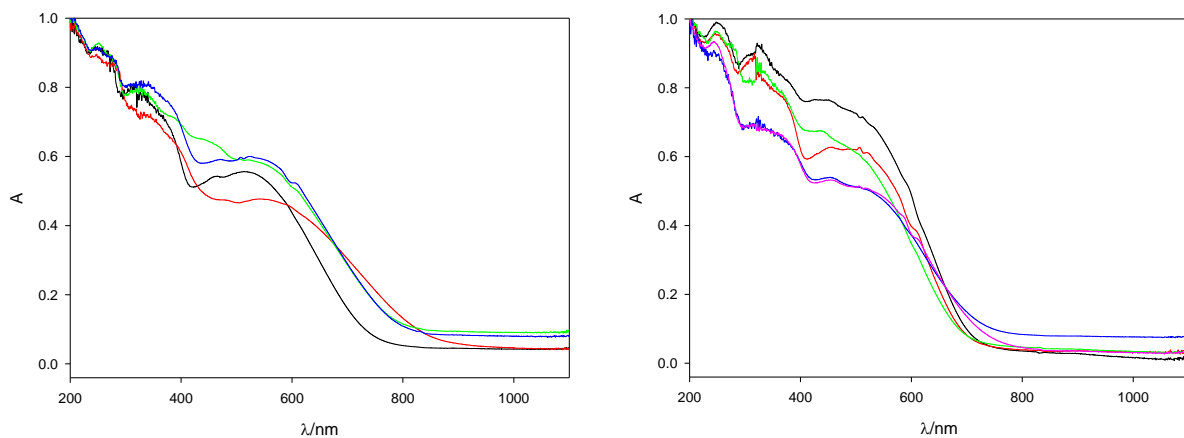


Fig. S13 Left: UV-VIS spectra of **C1** (black), **C2** (red), **C3** (green) and **C4** (blue). Right: UV-VIS spectra of **C5** (black), **C6** (red), **C7** (green), **C8** (blue) and **C9** (pink).

S4 ^1H and ^{13}C NMR spectroscopy of reported compounds

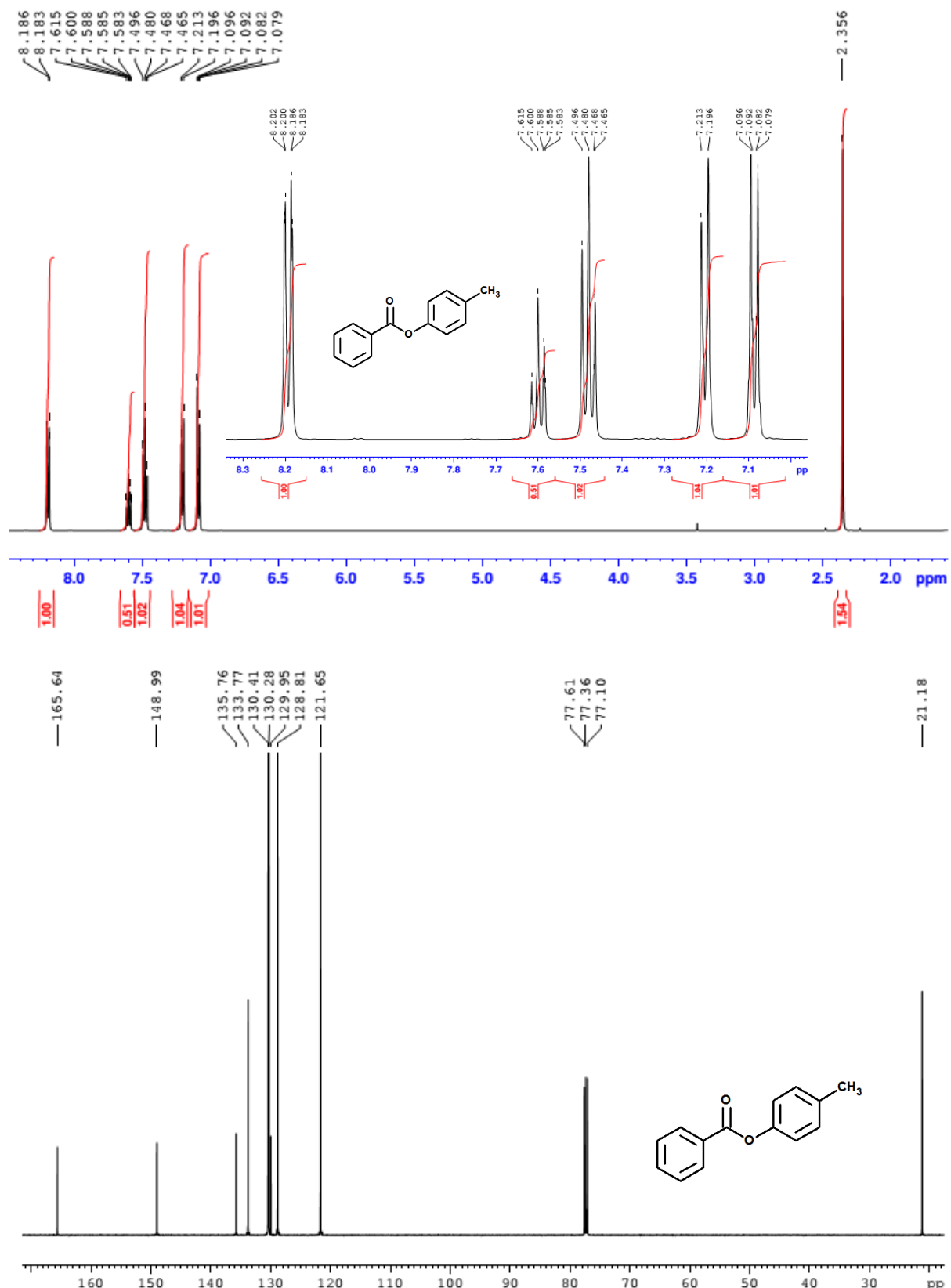


Fig. S14 ^1H NMR (upper) and ^{13}C NMR spektra of **3a**

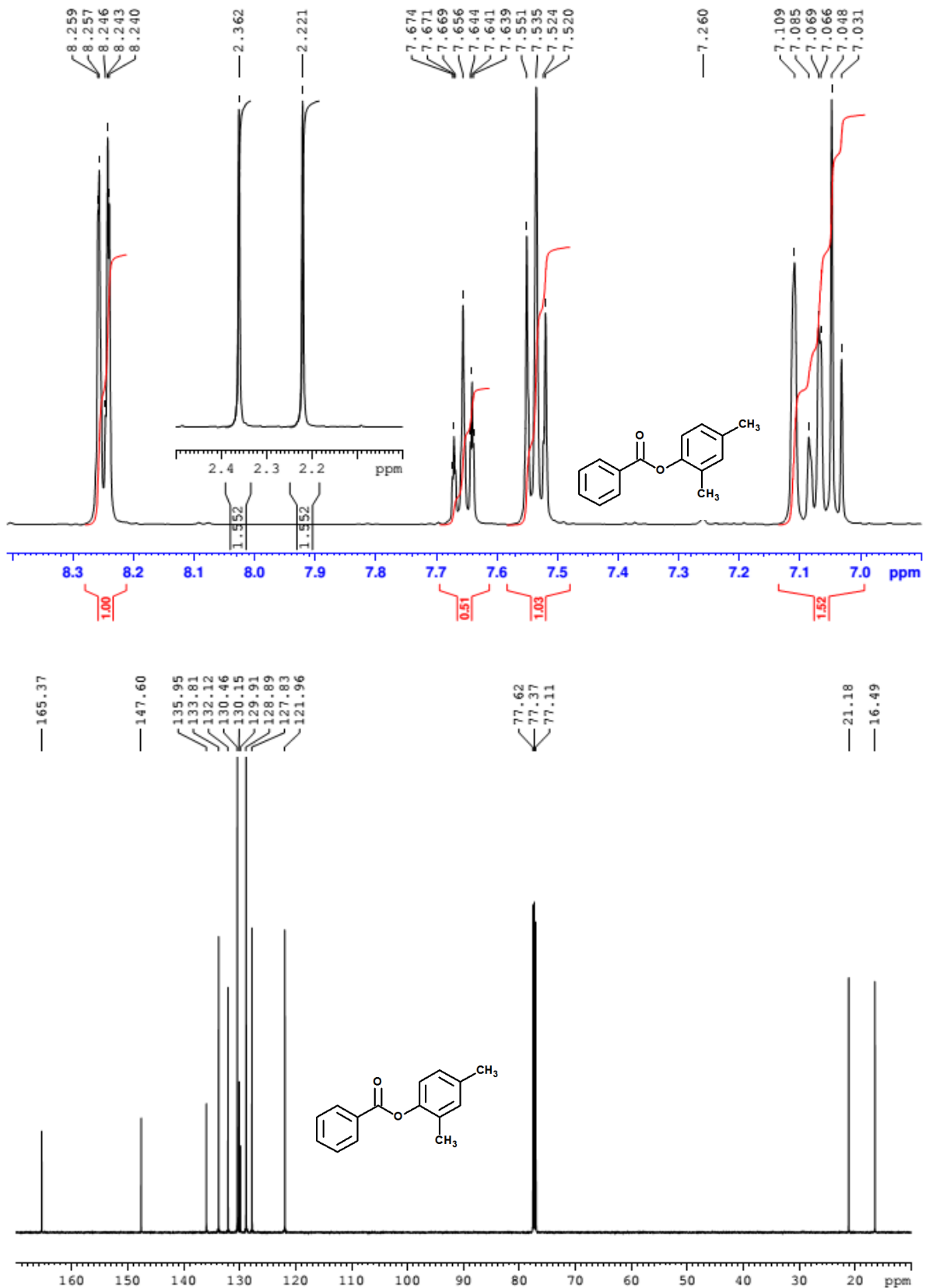


Fig. S15 ¹H NMR (upper) and ¹³C NMR spektra (bottom) of **3b**

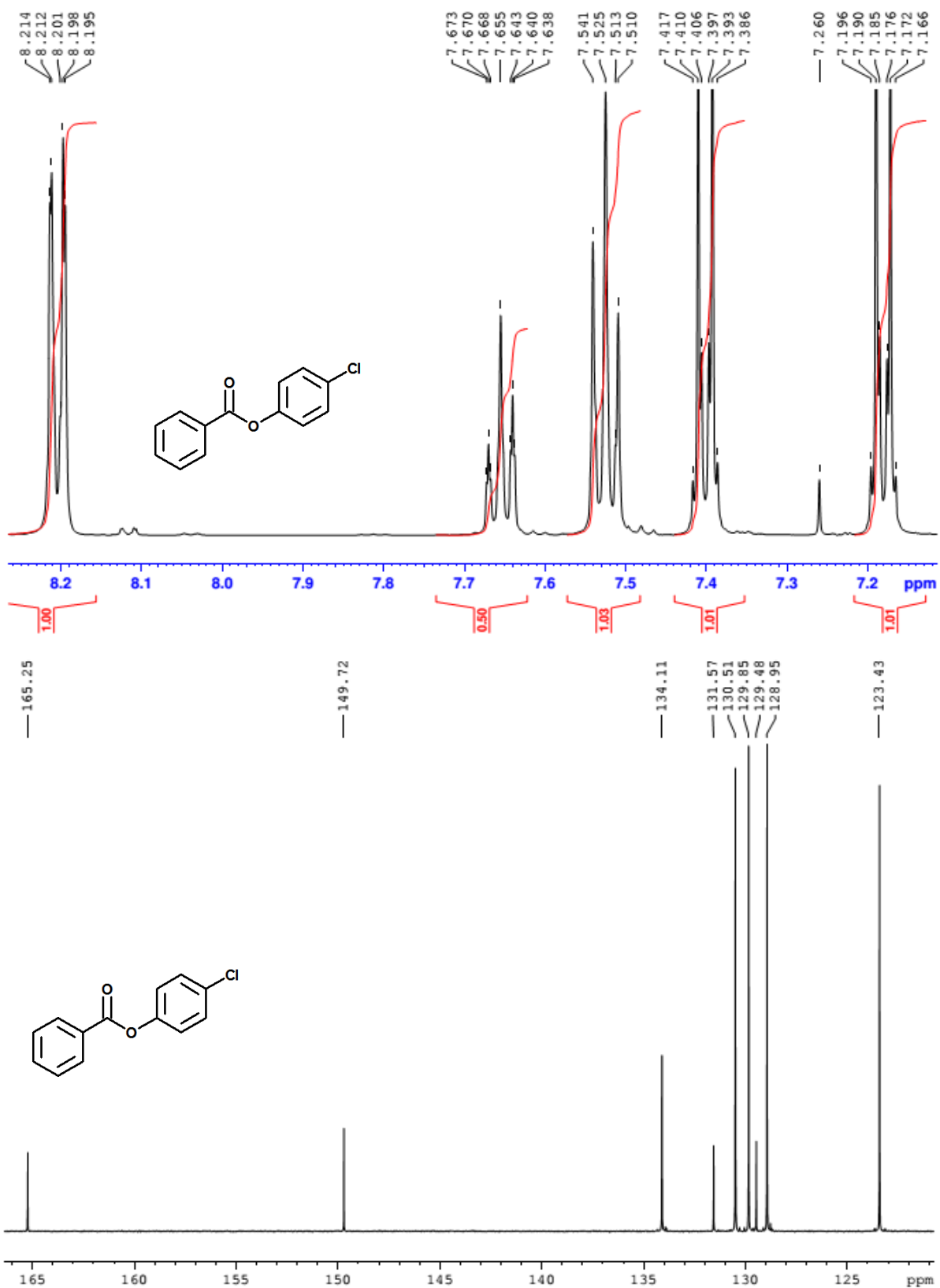


Fig. S16 ^1H NMR (upper) and ^{13}C NMR spektra (bottom) of **3c**

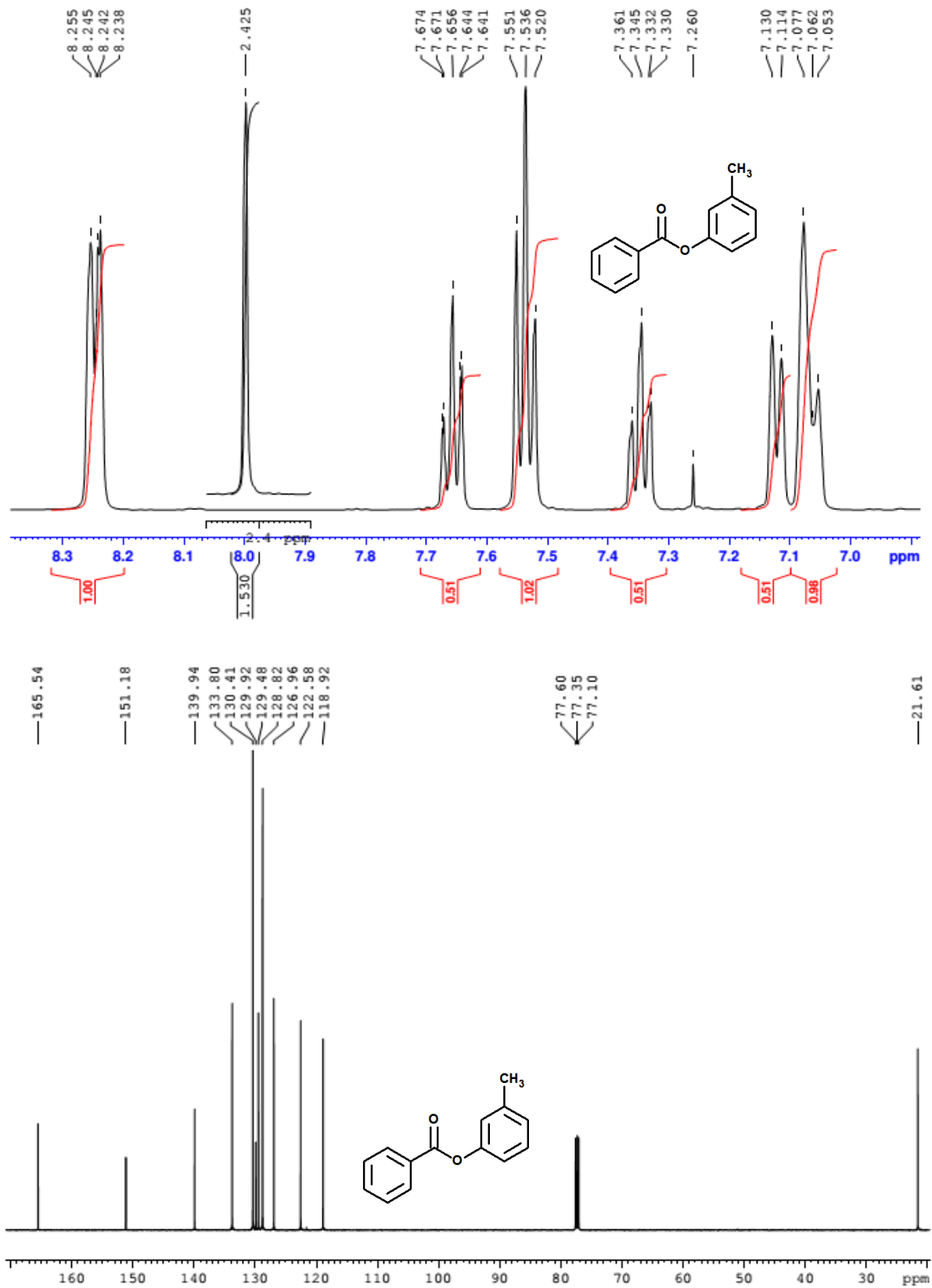


Fig. S17 ^1H NMR (upper) and ^{13}C NMR spektra (bottom) of **3d**

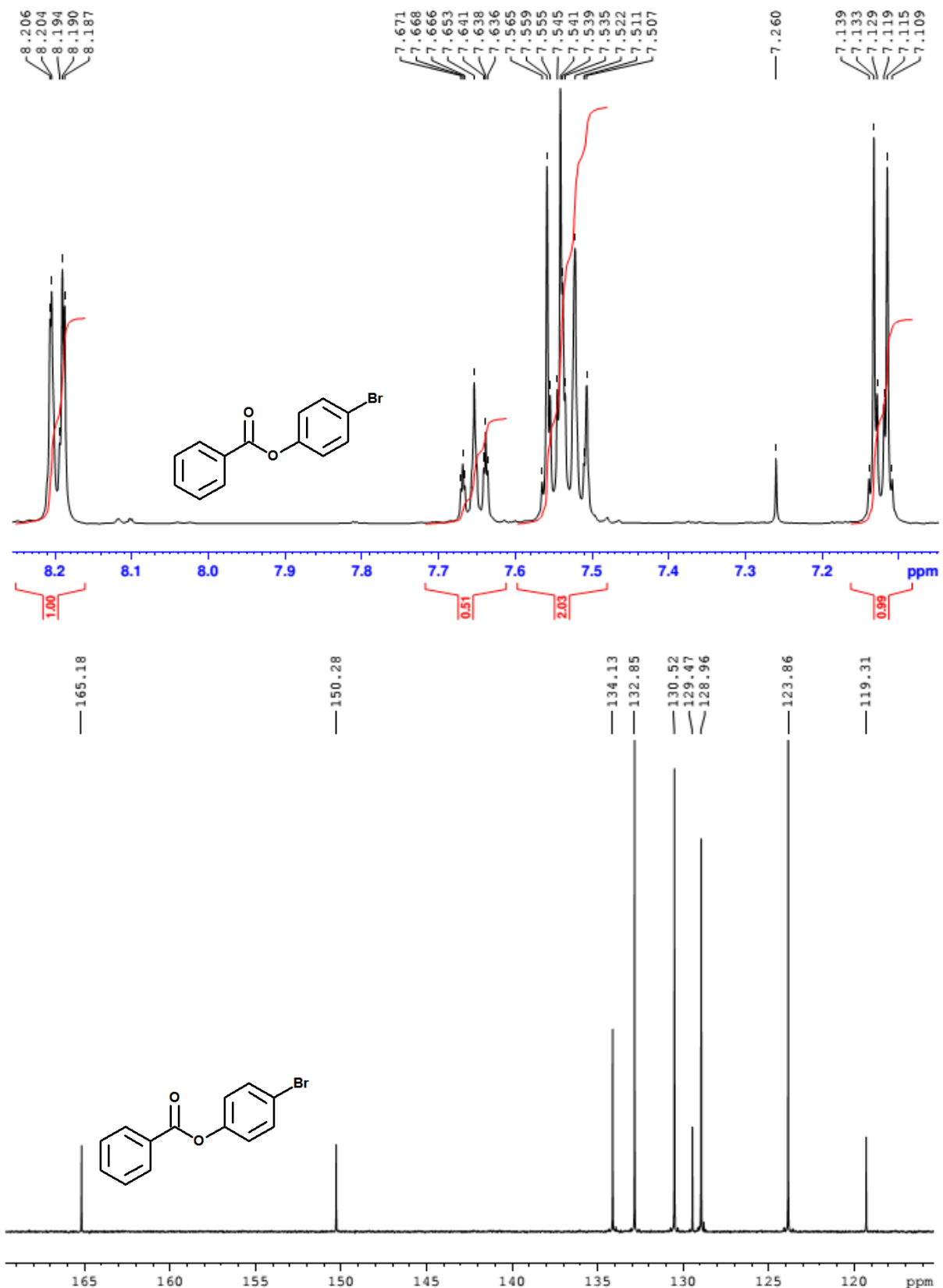


Fig. S18 ^1H NMR (upper) and ^{13}C NMR spektra (bottom) of **3e**

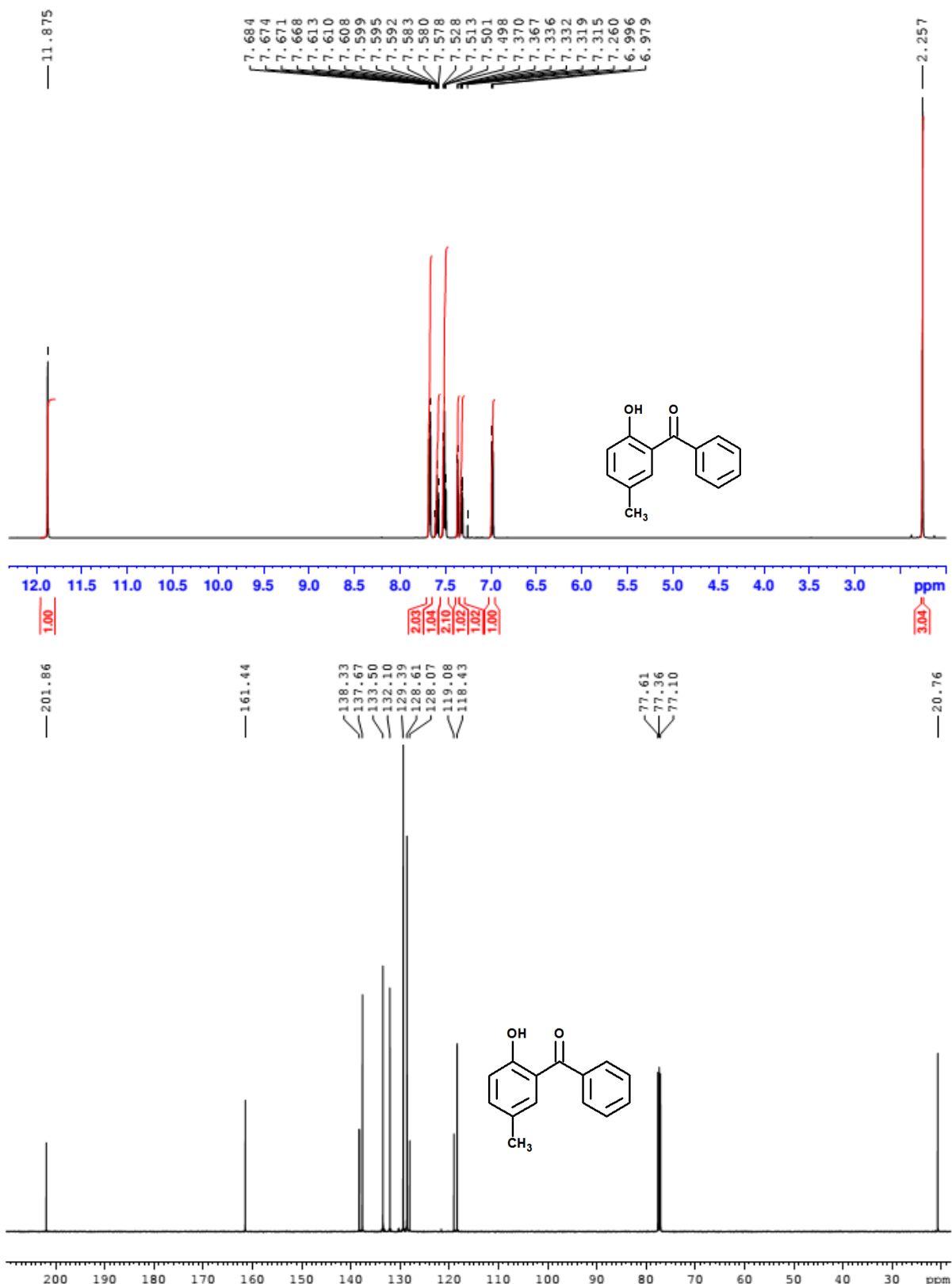


Fig. S19 ¹H NMR (upper) and ¹³C NMR spektra (bottom) of **4a**

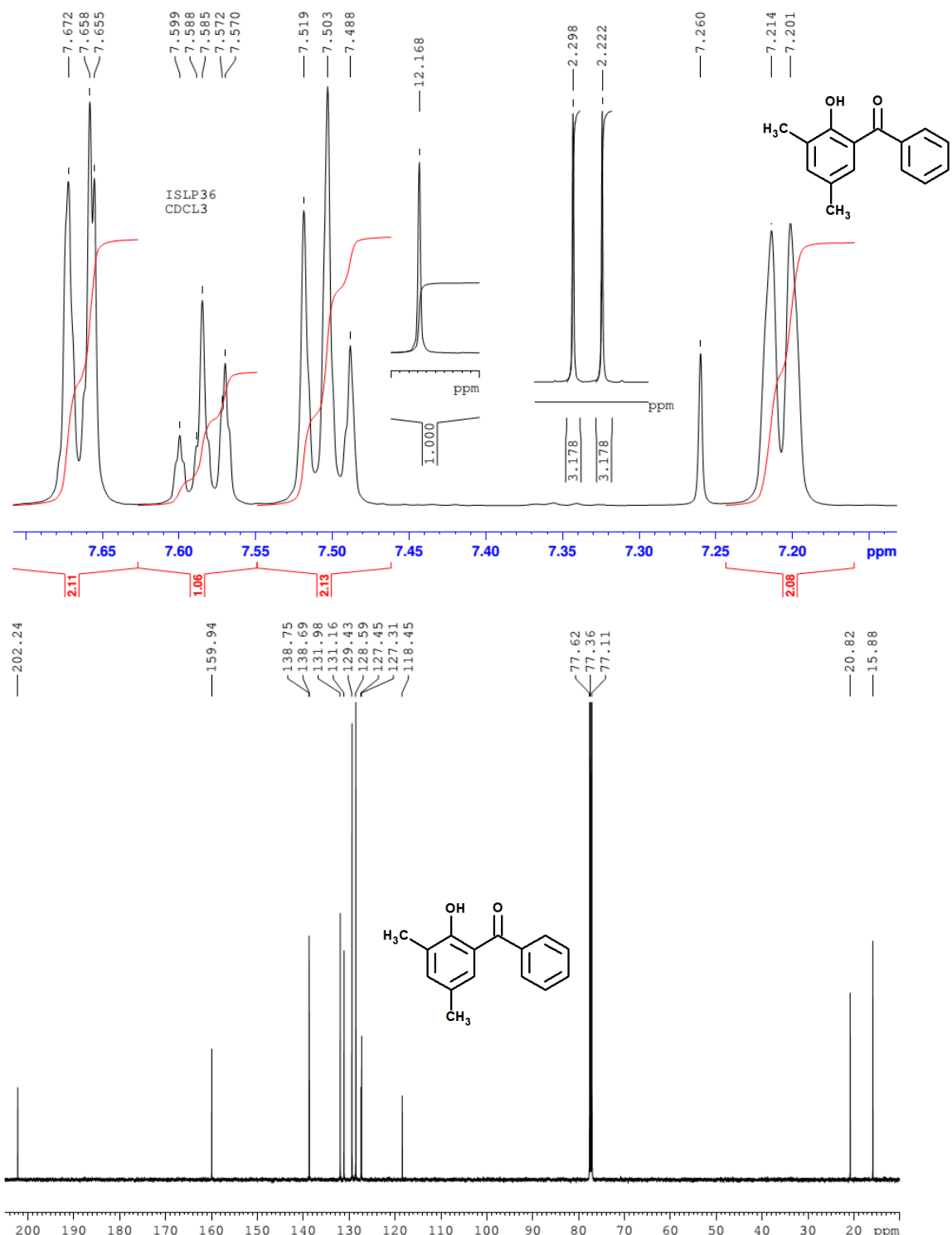


Fig. S20 ¹H NMR (upper) and ¹³C NMR spektra (bottom) of **4b**

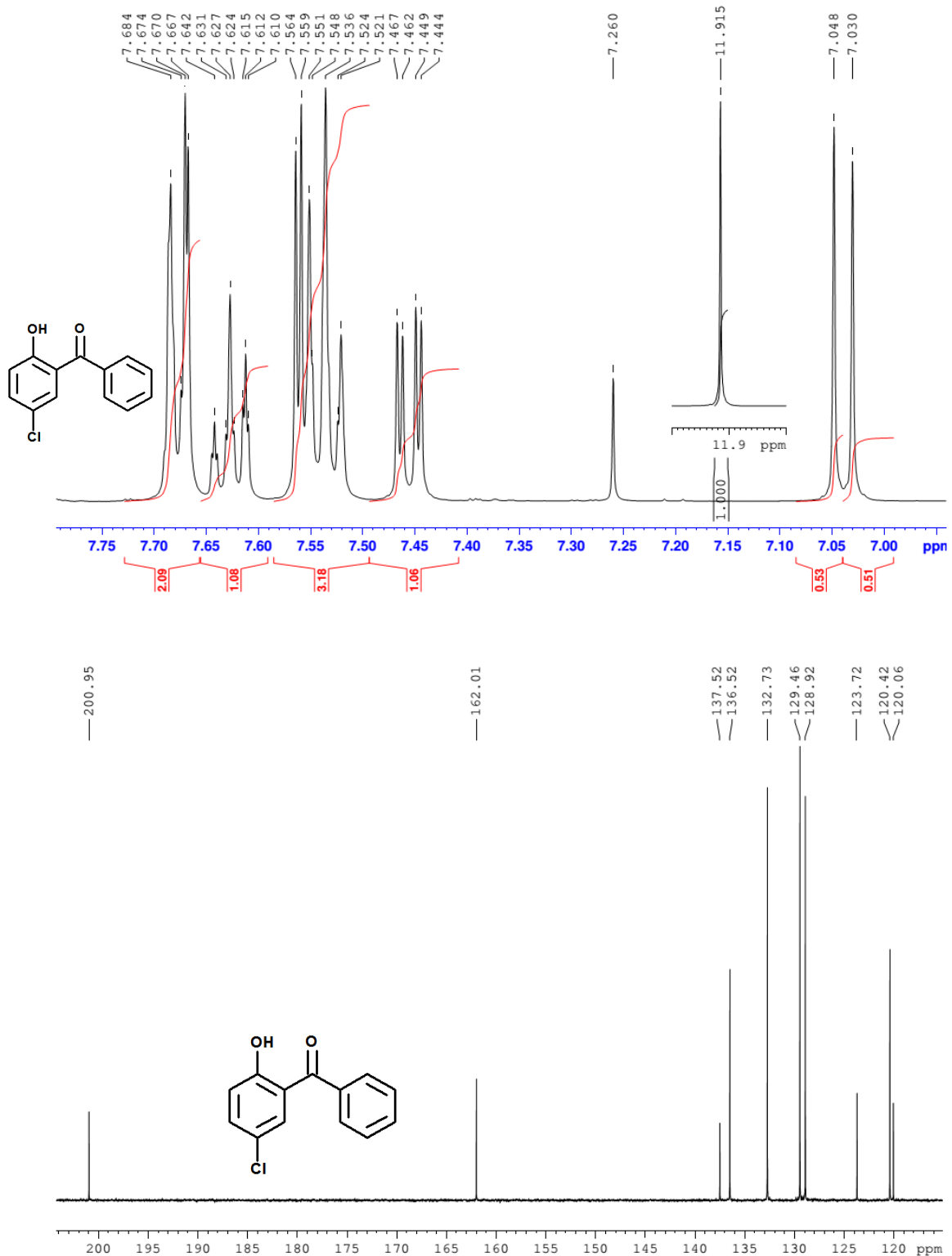


Fig. S21 ^1H NMR (upper) and ^{13}C NMR spektra (bottom) of **4c**

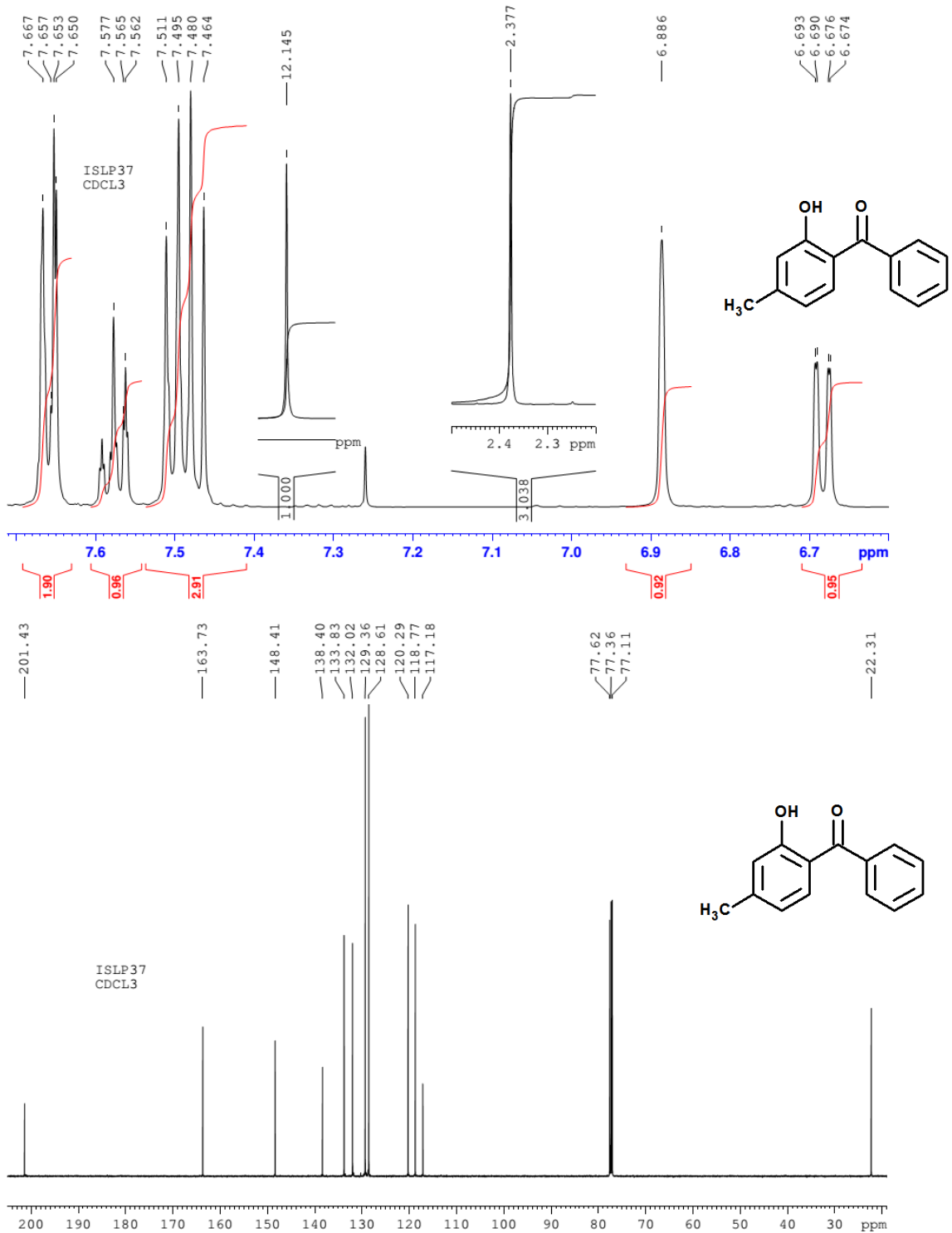


Fig. S22 ¹H NMR (upper) and ¹³C NMR spektra (bottom) of **4d**

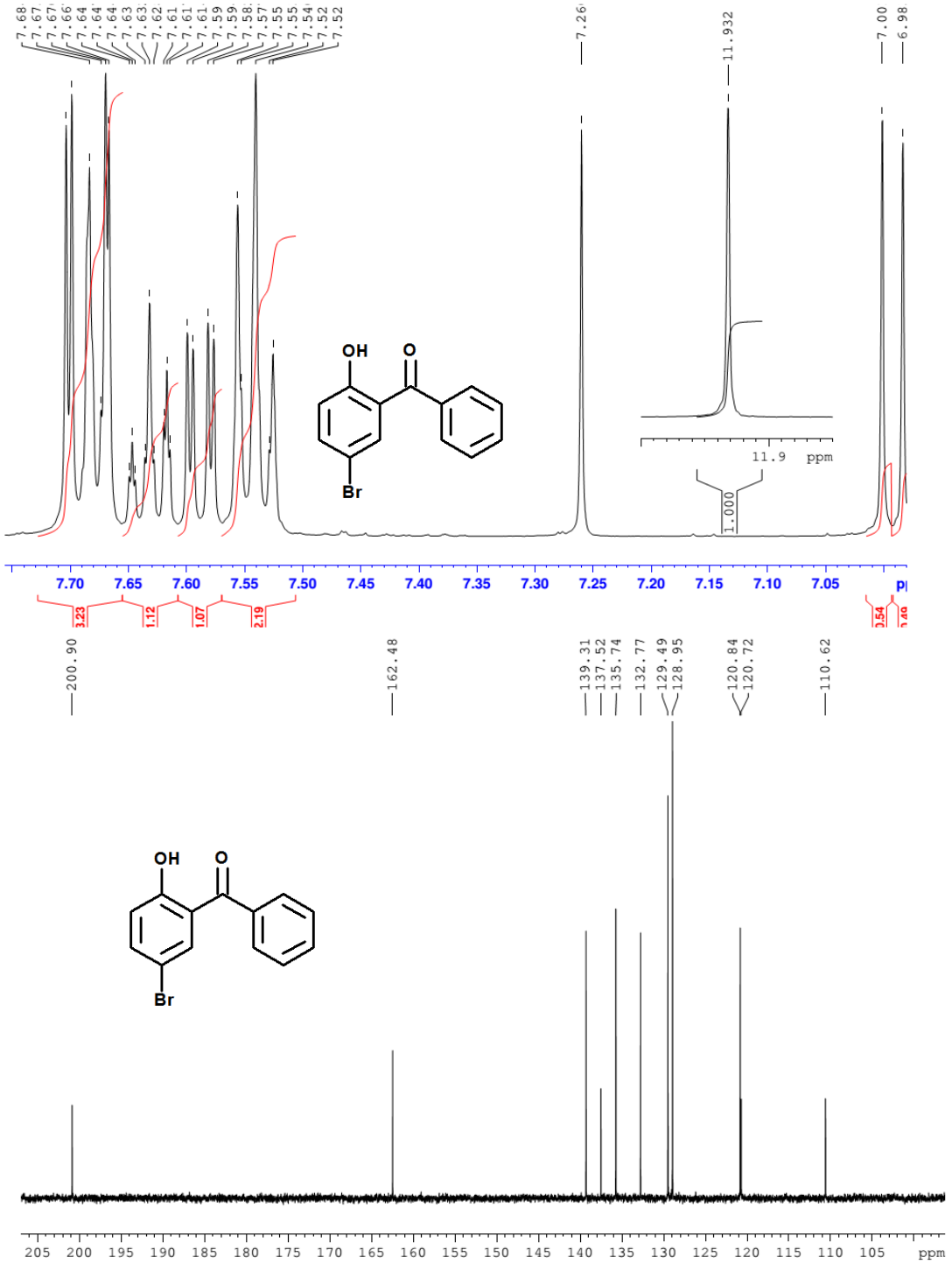


Fig. S23 ¹H NMR (upper) and ¹³C NMR spektra (bottom) of **4e**

S5 Bond angles and metric parameter of coordination polyhedra

Tab. S2 Selected bond lengths for the reported compounds

<i>Bond angles</i>	C1	C2	C3	C4	C5	C6	C7	C8A*	C8B*	C9
O1-Fe1-O2	88.18(7)°	89.86(5)°	89.21(4)°	89.75(5)°	88.05(9)°	89.08(6)°	93.23(5)°	174.06(8)°	174.06(8)°	176.05(7)°
O1-Fe1-N1	88.37(7)°	83.92(5)°	81.24(4)°	81.20(5)°	84.01(10)°	81.53(6)°	84.79(5)°	85.00(8)°	85.00(8)°	84.82(7)°
O1-Fe1-N2	107.35(7)°	158.94(5)°	108.96(4)°	108.79(5)°	161.39(10)°	107.42(6)°	160.64(5)°	83.1(3)°	91.4(3)°	87.51(7)°
O1-Fe1-N3	166.53(7)°	96.53(5)°	164.34(4)°	164.67(5)°	99.31(10)°	165.87(6)°	96.07(5)°	94.22(7)°	94.22(7)°	95.16(7)°
O2-Fe1-N1	100.22(7)°	170.58(5)°	101.80(4)°	99.45(5)°	165.57(10)°	96.28(6)°	170.36(5)°	94.65(8)°	94.65(8)°	93.58(7)°
O2-Fe1-N2	161.26(7)°	108.27(5)°	161.04(4)°	159.87(5)°	109.12(10)°	160.63(6)°	103.60(5)°	91.0(3)°	82.7(3)°	88.79(7)°
O2-Fe1-N3	87.25(7)°	82.20(5)°	83.26(4)°	83.05(5)°	82.16(10)°	84.30(6)°	83.05(5)°	85.05(7)°	85.05(7)°	85.71(7)°
N3-Fe1-N1	79.99(7)°	91.46(5)°	86.86(4)°	86.65(5)°	87.25(10)°	86.79(6)°	87.78(6)°	169.54(8)°	169.54(8)°	168.85(7)°
N1-Fe1-N2	70.57(7)°	76.68(5)°	76.50(4)°	76.50(5)°	77.67(10)°	76.78(6)°	77.03(6)°	84.92(19)°	88.83(19)°	86.16(8)°
N3-Fe1-N2	75.24(7)°	76.08(5)°	77.79(4)°	77.07(5)°	76.74(10)°	77.33(6)°	76.86(6)°	84.63(19)°	80.77(19)°	82.70(7)°
O1-Fe1-X1	88.85(5)°	104.02(4)°	95.38(5)°	94.75(5)°	101.92(11)°	95.50(7)°	99.34(6)°	93.37(8)°	93.37(8)°	92.66(8)°
O2-Fe1-X1	97.37(5)°	91.11(3)°	101.91(5)°	101.32(5)°	94.82(11)°	101.96(7)°	92.31(6)°	92.56(9)°	92.56(9)°	91.14(8)°
N1-Fe1-X1	162.09(6)°	97.24(4)°	155.99(5)°	158.81(5)°	98.59(11)°	161.48(7)°	97.32(6)°	96.74(9)°	96.74(9)°	97.88(9)°
N2-Fe1-X1	93.45(5)°	86.69(4)°	82.27(5)°	85.31(6)°	84.22(11)°	86.82(7)°	89.60(6)°	175.9(2)°	173.0(3)°	175.95(9)°
N3-Fe1-X1	104.30(5)°	158.38(4)°	99.59(5)°	99.91(5)°	158.45(12)°	98.08(7)°	164.14(6)°	93.71(9)°	93.71(9)°	93.26(8)°
$\Sigma /^\circ$	104	93	111	105	104	97	83	54	54	48
$\Theta /^\circ$	226	243	262	244	241	221	185	68	77	82

*occupancy factor A=0.493(3) B=0.507(3)

Tab. S3 Parameters of N2–H2…O1 hydrogen bonds for **C1–C7**

	$d(\text{N2–H2}) / \text{\AA}$	$d(\text{H2–O1}) / \text{\AA}$	$d(\text{N2–O1}) / \text{\AA}$	$\text{N2–H2–O1} / {}^\circ$	Symmetry codes
C1	1.00	1.87	2.838(2)	161	-x, 3-y, -z
C2	1.00	1.90	2.896(2)	171	-x, 1-y, -z
C3	1.00	1.98	2.970(2)	170	1-x, 2-y, 1-z
C4	1.00	2.04	3.022(2)	167	1-x, 3-y, 1-z
C5	1.00	1.89	2.861(3)	163	1-x, 2-y, 1-z
C6	1.00	1.88	2.864(2)	167	1-x, 2-y, 1-z
C7	1.00	2.13	2.984(2)	142	1-x, 1-y, 1-z

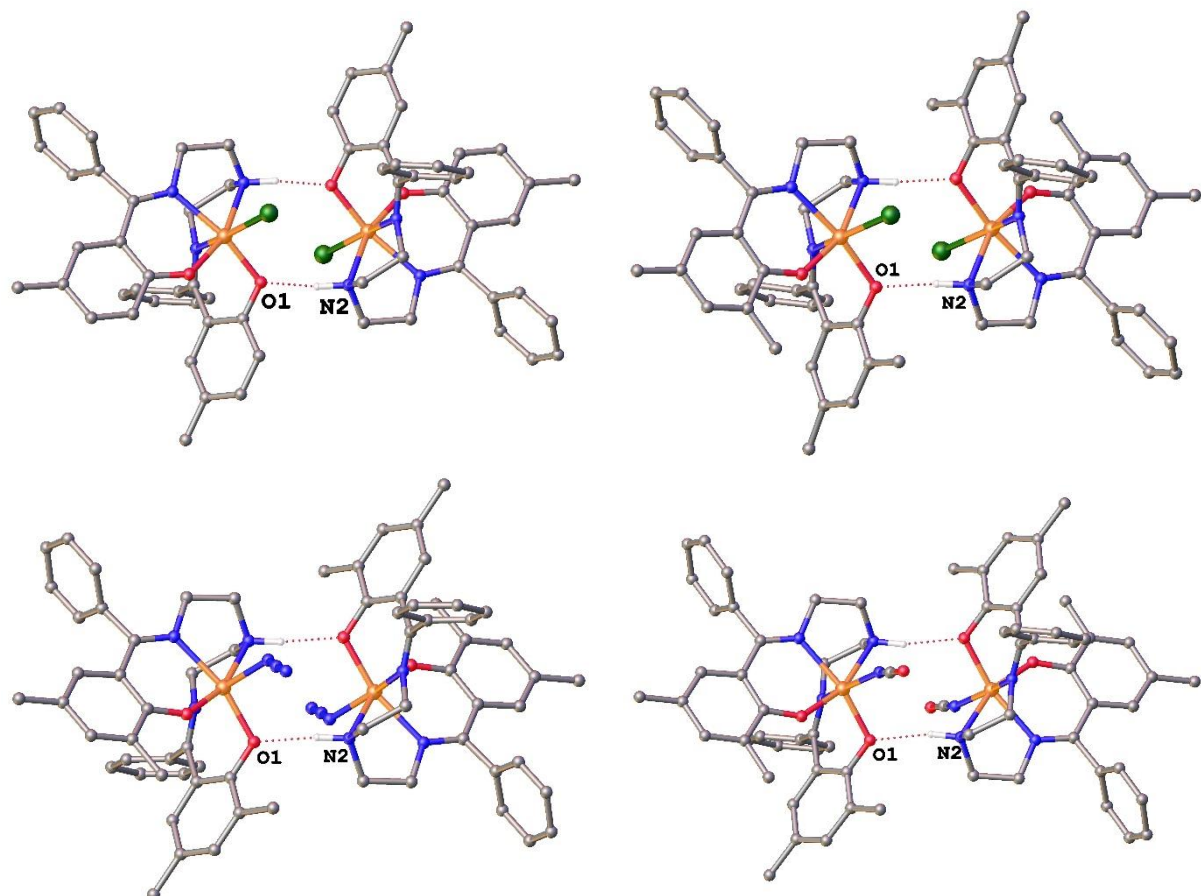


Fig. S24 Formation of supramolecular dimers in crystal structure of **C1** (upper left), **C2** (upper right), **C3** (middle left) and **C4** (middle right). Hydrogens are omitted for clarity.

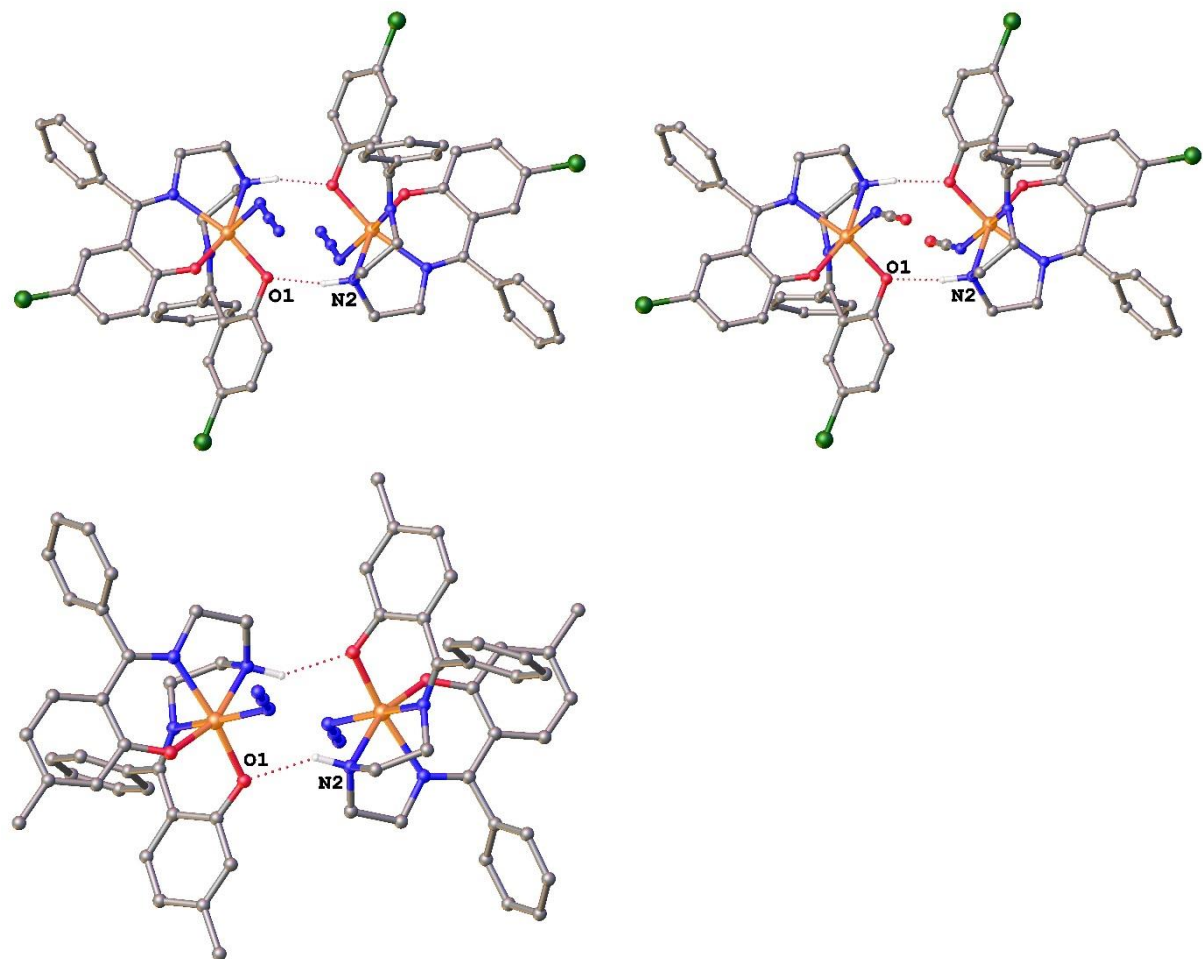


Fig. S25 Formation of supramolecular dimers in crystal structure of **C5** (upper left), **C6** (upper right) and **C7** (bottom left). Hydrogens are omitted for clarity.

Tab. S4 The $\text{Fe1}\cdots\text{Fe1}$ distances of supramolecular dimmers for **C1–C7**

	$d(\text{Fe1–Fe1}) / \text{\AA}$	Symmetry codes
C1	5.123(1)	-x, 3-y, -z
C2	5.088(1)	-x, 1-y, -z
C3	5.043(1)	1-x, 2-y, 1-z
C4	5.100(1)	1-x, 3-y, 1-z
C5	4.986(1)	1-x, 2-y, 1-z
C6	5.025(1)	1-x, 2-y, 1-z
C7	4.945(1)	1-x, 1-y, 1-z

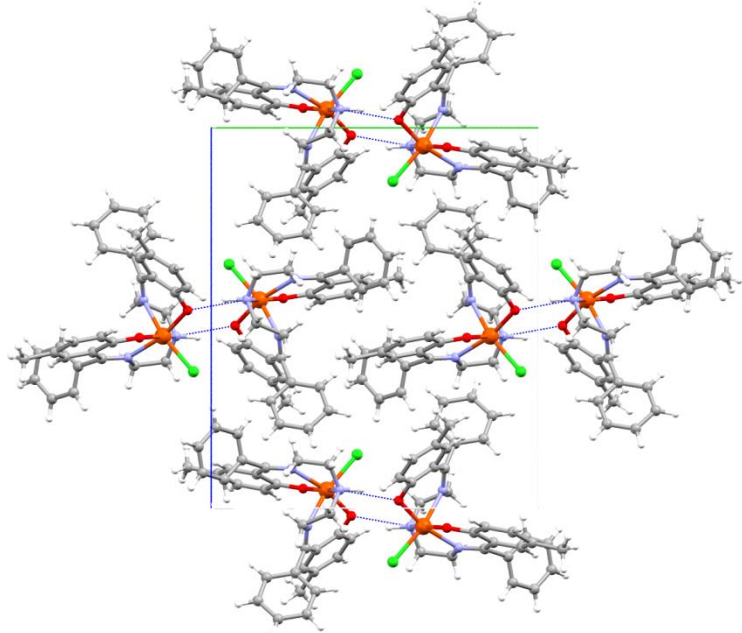


Fig. S26 The crystal packing of C1

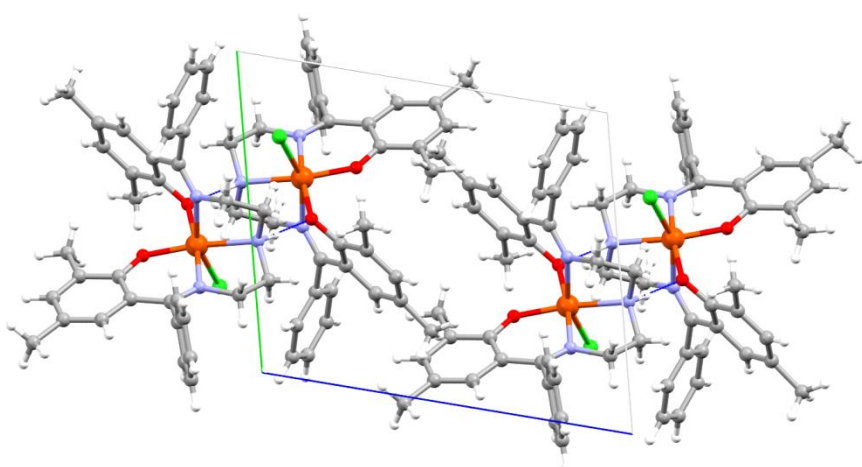


Fig. S27 The crystal packing of C2

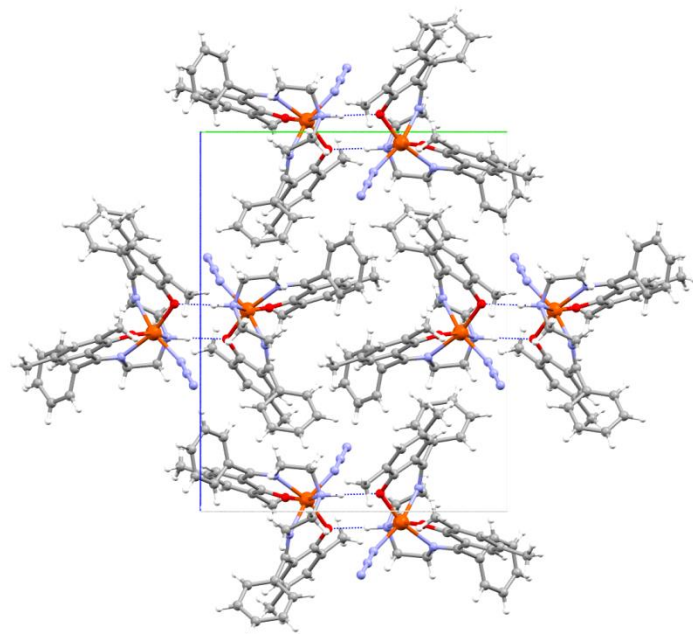


Fig. S28 The crystal packing of **C3**

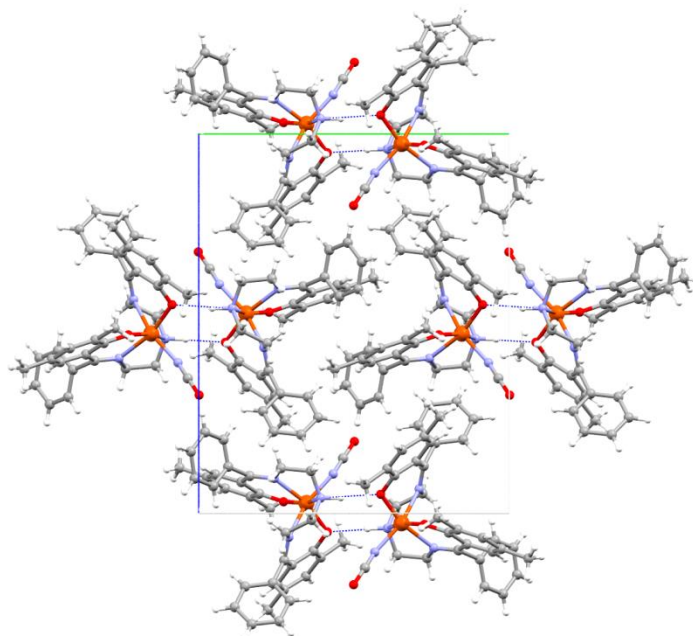


Fig. S29 The crystal packing of **C4**

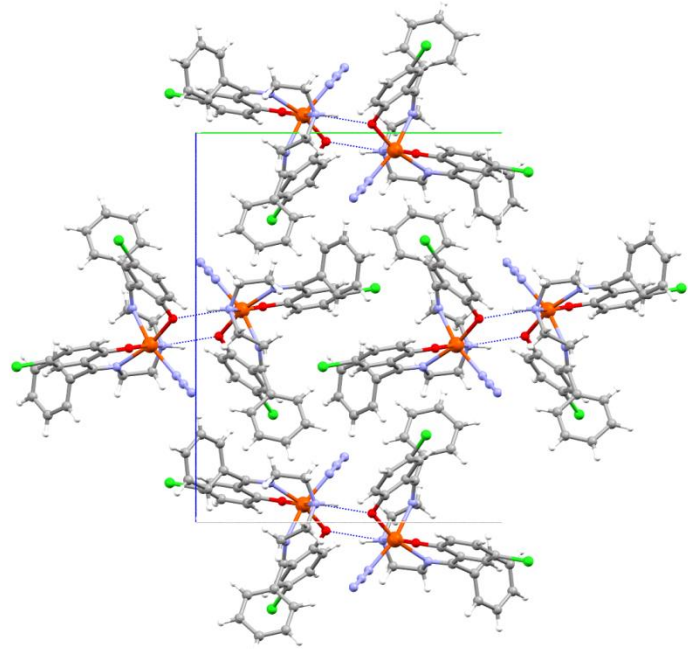


Fig. S30 The crystal packing of C5

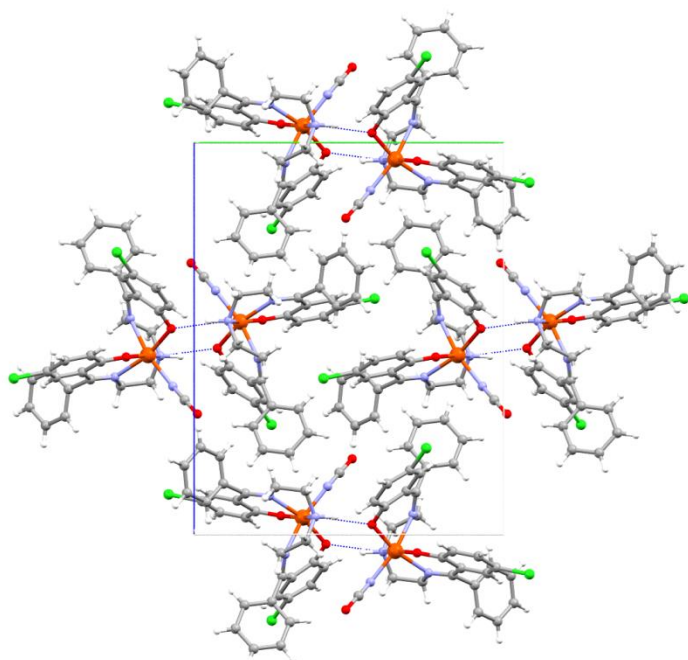


Fig. S31 The crystal packing of C6

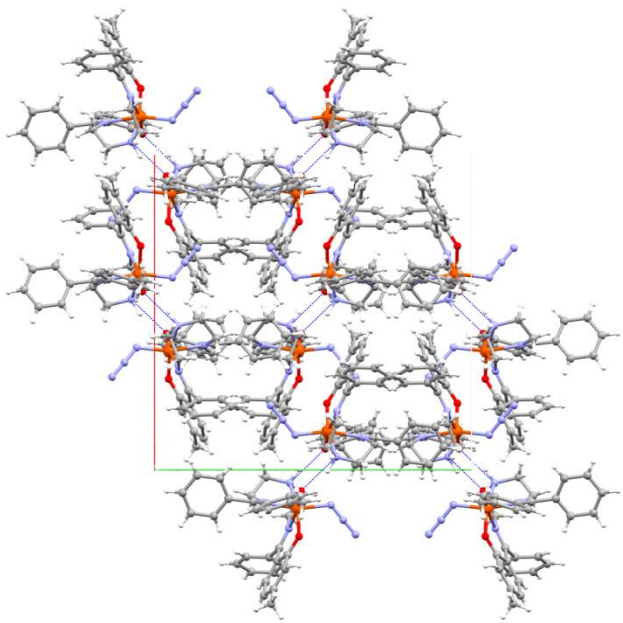


Fig. S32 The crystal packing of C7

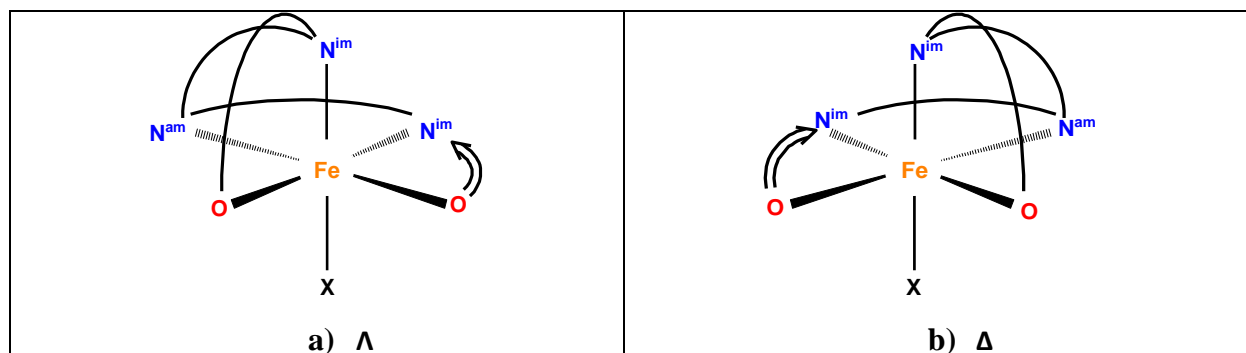


Fig. S33 Two possible isomeric forms of fac-N₃, cis-O₂ configuration of mononuclear complexes with Schiff base ligands containing N,N-bis(ethylene)amine aliphatic part

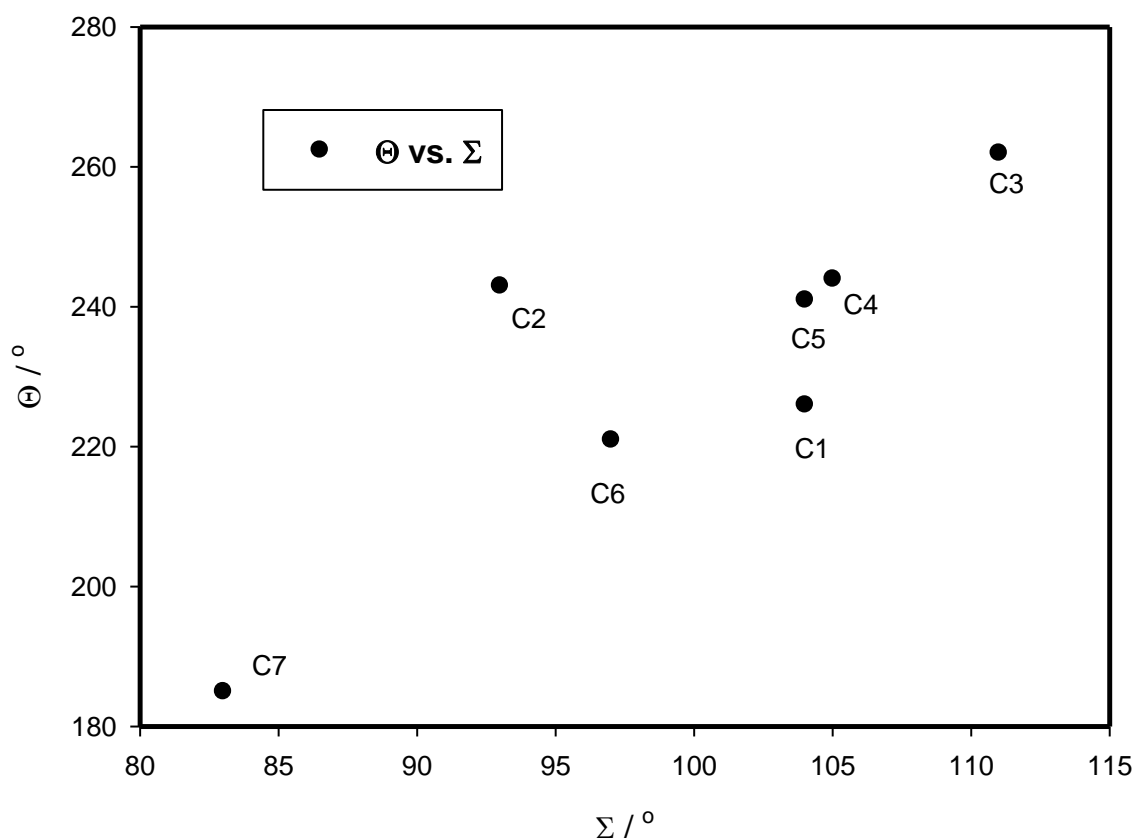
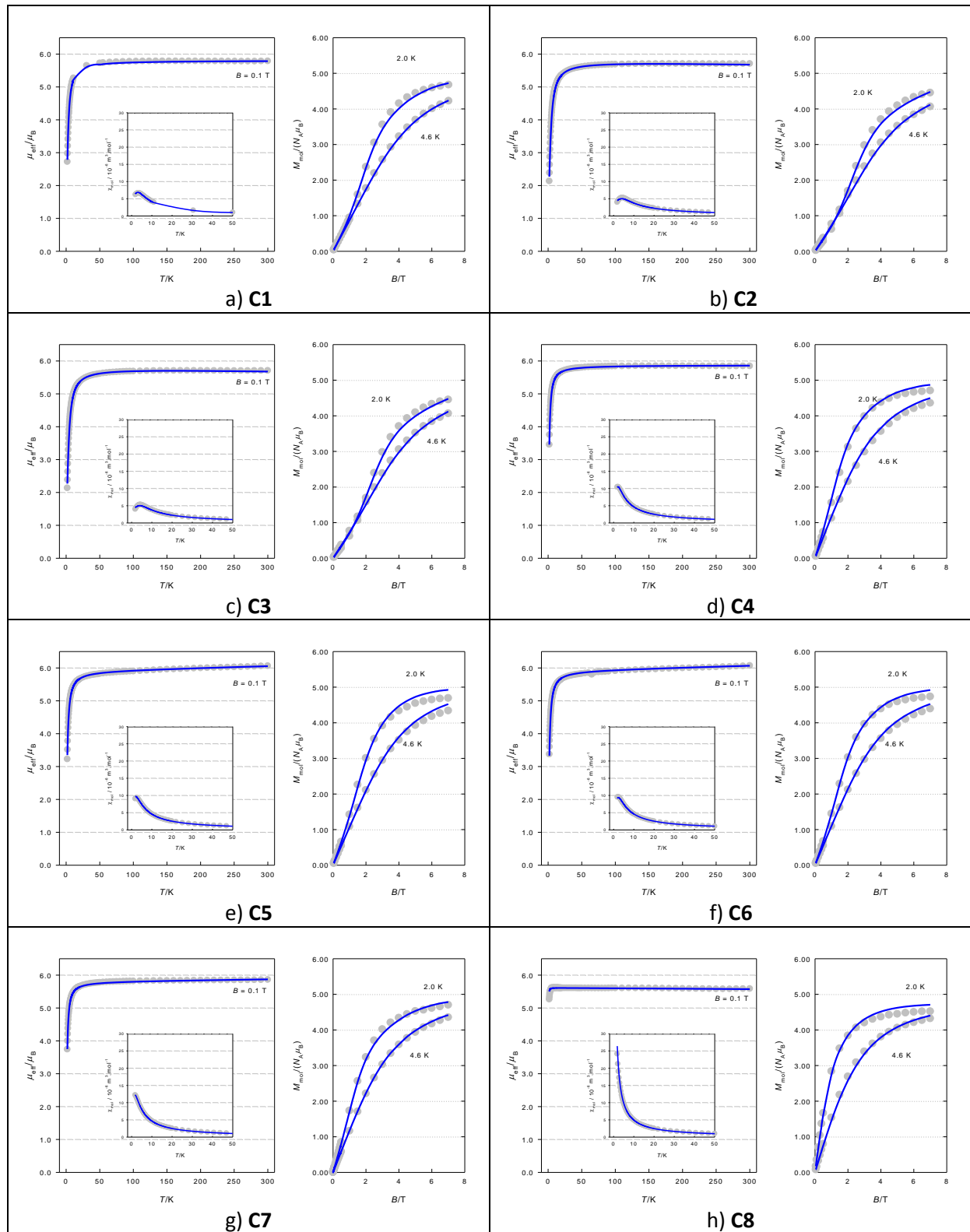


Fig. S34 Correlation between two distortion parameters Θ and Σ for compound **C1-C7** which have *cis*-O₂, fac-N₃ conformation of coordination polyhedral. $\Sigma = \sum_{i=1}^{12}(|\varphi_i - 90|)$; where φ_i is value of N-Fe-N octahedron angle. $\Theta = \sum_{i=1}^{24}(|\theta_i - 60|)$; where θ_i are 24 angles measured on the projection of two triangular faces of the octahedron along their common pseudo-threecold axis. a) P. Guionneau, M. Marchivie, G. Bravic, J. F. Létard, D. Chasseau, *Top. Curr. Chem.*, 2004, **234**, 97. b) M. A. Halcrow *Chem. Soc. Rev.*, 2011, 40, 4119–4142.

S6 Magnetic functions and their theoretical analyses



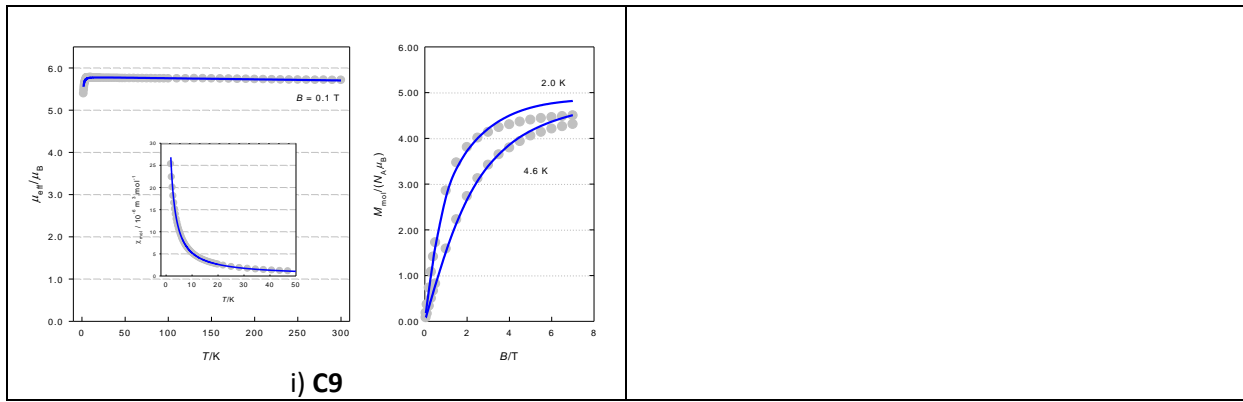


Fig. S35 Magnetic functions for **C1-C9** and their theoretical analysis with D(+) alternative, effective magnetic moment *vs* temperature (left), magnetization *vs* magnetic field (right), magnetic susceptibility *vs* temperature (inset); grey circles: experimental data, solid line: fitted.

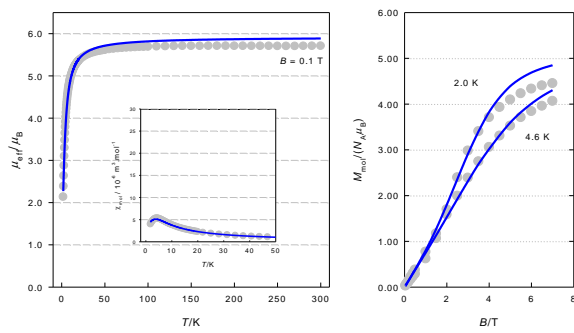


Fig. S36 Magnetic functions for **C2** and their theoretical analysis without *D* parameter including the effect of molecular field (parameter *zJ*); effective magnetic moment *vs* temperature (left), magnetization *vs* magnetic field (right), magnetic susceptibility *vs* temperature (inset); grey circles: experimental data, solid line: fitted. The optimum parameter values are $J=-0.719 \text{ cm}^{-1}$, $g=2.00$, $zJ=-0.099 \text{ cm}^{-1}$, $R(\chi)=0.040$, $R(M)=0.060$.

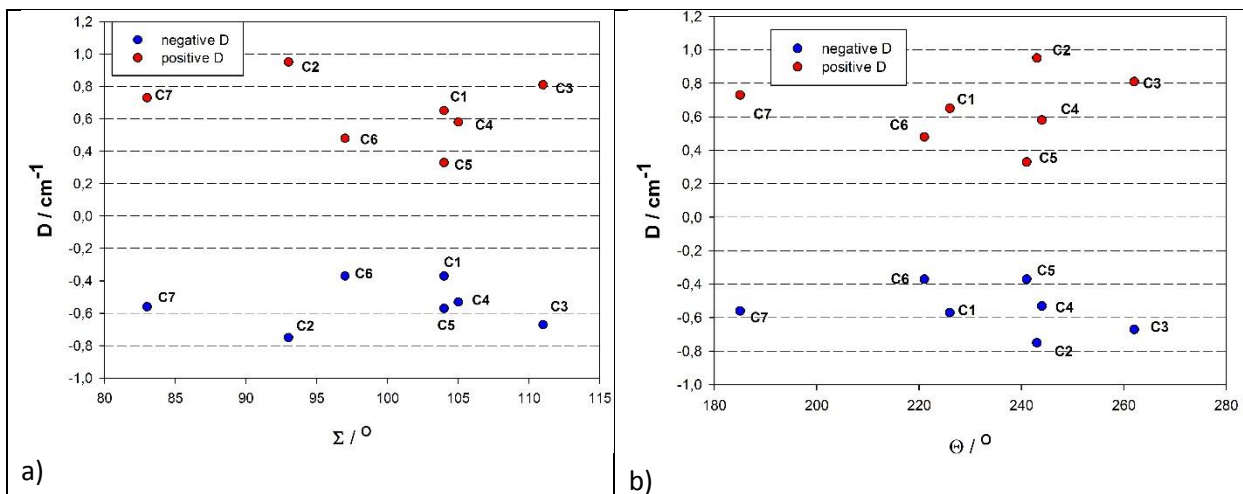


Fig. S37 Correlation between axial parameter of zero field splitting *D* with distortion parameters Θ and Σ for compound **C1-C9**